Molecular Plant Pathology

MOLECULAR PLANT PATHOLOGY (2018) 19(6), 1427–1443 DOI: 10.1111/mpp.12626

Phosphorylation coexists with *O*-GlcNAcylation in a plant virus protein and influences viral infection

SANDRA MARTÍNEZ-TURIÑO[1,*], JOSÉ DE JESÚS PÉREZ[1†], MARTA HERVÁS[1], ROSANA NAVAJAS[2], SERGIO CIORDIA[2], NAMRATA D. UDESHI[3‡], JEFFREY SHABANOWITZ[3], DONALD F. HUNT[3] AND JUAN ANTONIO GARCÍA[1,*]

[1]*Department of Plant Molecular Genetics, Centro Nacional de Biotecnología (CNB-CSIC), Campus Universidad Autónoma de Madrid, Madrid 28049, Spain*
[2]*Proteomics Unit, Centro Nacional de Biotecnología (CNB-CSIC), ProteoRed ISCIII, Madrid 28049, Spain*
[3]*Department of Chemistry, University of Virginia, Charlottesville VA 22904, USA*

SUMMARY

Phosphorylation and *O*-GlcNAcylation are two widespread post-translational modifications (PTMs), often affecting the same eukaryotic target protein. *Plum pox virus* (PPV) is a member of the genus *Potyvirus* which infects a wide range of plant species. *O*-GlcNAcylation of the capsid protein (CP) of PPV has been studied extensively, and some evidence of CP phosphorylation has also been reported. Here, we use proteomics analyses to demonstrate that PPV CP is phosphorylated *in vivo* at the N-terminus and the beginning of the core region. In contrast with the 'yin–yang' mechanism that applies to some mammalian proteins, PPV CP phosphorylation affects residues different from those that are *O*-GlcNAcylated (serines Ser-25, Ser-81, Ser-101 and Ser-118). Our findings show that PPV CP can be concurrently phosphorylated and *O*-GlcNAcylated at nearby residues. However, an analysis using a differential proteomics strategy based on iTRAQ (isobaric tags for relative and absolute quantitation) showed a significant enhancement of phosphorylation at Ser-25 in virions recovered from *O*-GlcNAcylation-deficient plants, suggesting that crosstalk between *O*-GlcNAcylation and phosphorylation in PPV CP takes place. Although the preclusion of phosphorylation at the four identified phosphotarget sites only had a limited impact on viral infection, the mimicking of phosphorylation prevents PPV infection in *Prunus persica* and weakens infection in *Nicotiana benthamiana* and other herbaceous hosts, prompting the emergence of potentially compensatory second mutations. We postulate that the joint action of phosphorylation and *O*-GlcNAcylation in the N-proximal segment of CP allows a fine-tuning of protein stability, providing the amount of CP required in each step of viral infection.

**Correspondence*: Email: jagarcia@cnb.csic.es; sandra.martinez@cnb.csic.es
†*Present address*: División de Biología Molecular, Instituto Potosino de Investigación Científica y Tecnológica A.C., Camino a la Presa San José 2055, San Luis Potosí, SLP, México
‡*Present address*: Proteomics Platform, The Broad Institute of MIT and Harvard, 7 Cambridge Center, Room 5033, Cambridge MA 02142, USA

Keywords: Coat protein, crosstalk, *O*-GlcNAcylation, phosphorylation, *Plum pox virus*, *Potyvirus*, yin-yang.

INTRODUCTION

Cellular proteins often bear various post-translational modifications (PTMs), including glycosylation and phosphorylation, which regulate processes involved in numerous biological functions. Unlike classical *N*- or *O*-linked glycosylation, which attaches complex oligosaccharide chains to proteins directed to the secretory pathway, another form of glycosylation, *O*-GlcNAcylation, attaches single β-*N*-acetylglucosamine residues to serine (Ser) and/or threonine (Thr) side-chains through an *O*-β-glycosidic bond (*O*-GlcNAc) (Hart, 1997). *O*-GlcNAcylated proteins are usually also phosphorylated (Slawson and Hart, 2003). *O*-GlcNAcylation and phosphorylation are rapidly cycling PTMs and often show extensive, complex interplay (Butkinaree *et al.*, 2010; Zeidan and Hart, 2010). These modifications can compete for the same Thr or Ser residue. They can also occupy adjacent or distant sites; in this case, they can establish positive or negative interactions, or be mutually independent. Moreover, enzymes involved in *O*-GlcNAcylation and phosphorylation are themselves regulated by these PTMs, and interact in multiprotein complexes (Zeidan and Hart, 2010).

Although phosphorylation has been studied extensively in animals and plants, research on *O*-GlcNAcylation in plants lags far behind that in other eukaryotic organisms (Olszewski *et al.*, 2010). This is reflected in the fact that, by the end of last year, just nine proteins of plant origin were included in the dbOGAP database (https://wangj27.u.hpc.mssm.edu/hulab/OGAP.html), which housed 1240 proteins reported as potentially *O*-GlcNAc modified (Wang *et al.*, 2011). Very recently, a high-throughput proteomics assay has identified 262 *O*-GlcNAcylated *Arabidopsis thaliana* proteins (Xu *et al.*, 2017), still a reduced number when compared with over 1000 proteins uncovered in different studies of mammalian cells (Hahne *et al.*, 2013; Trinidad *et al.*, 2012). Two *O*-GlcNAc transferases (OGTs) have been identified in the model plant *A. thaliana*: SPINDLY (SPY), which is similar to some

bacterial OGTs, and SECRET AGENT (SEC), which is similar to mammalian OGTs (Hartweck *et al.*, 2002). For a long time, the capsid protein (CP) of *Plum pox virus* (PPV), which is modified by SEC, was the only protein definitively identified as a natural target of a specific plant OGT (Chen *et al.*, 2005). Although there is sound evidence of functionally relevant *O*-GlcNAcylation in several plant proteins, such as the *Nicotiana tabacum* non-cell-autonomous pathway protein 1 (Nt-NCAPP1) and some phloem non-cell-autonomous proteins (NCAPs) of pumpkin (Taoka *et al.*, 2007), two *A. thaliana* TCP transcription factors, TCP14 and TCP15 (Steiner *et al.*, 2012), some lectin-interacting tobacco histones (Delporte *et al.*, 2014; Schouppe *et al.*, 2011) and the vernalization-related RNA-binding protein TaGRP2 of wheat (Xiao *et al.*, 2014; Xing *et al.*, 2009), the OGTs involved in these putative modifications have not been identified. Recently, SEC-mediated *O*-GlcNAcylation of several proteins of the DELLA family of transcription regulators has been demonstrated in Arabidopsis (Zentella *et al.*, 2016).

Although *O*-GlcNAcylated plant proteins are usually also phosphorylated, the relationship between *O*-GlcNAcylation and phosphorylation in plants has been little addressed. Analysis of a pumpkin NCAP, Cm-PP16-1, has suggested that a Ser residue that is phosphorylated *in vivo* is also a target of *O*-GlcNAc modification (Taoka *et al.*, 2007). Whereas DELLA protein phosphorylation is thought to increase their stability, *O*-GlcNAcylation by SEC represses DELLA activity; whether these modifications affect one another remains to be determined (Zentella *et al.*, 2016).

PPV is a member of the genus *Potyvirus* which, in nature, infects *Prunus* trees, although it can also infect experimental herbaceous hosts (García *et al.*, 2014; Šubr and Glasa, 2013). The potyvirus genome is a positive-sense, single-stranded RNA of ~10 kb encapsidated by a single type of CP to form flexuous rod particles. It is translated into a large polyprotein that is proteolytically processed to at least 10 final products (Revers and García, 2015). A frameshift resulting from RNA polymerase slippage allows the production of additional transframe products (Hagiwara-Komoda *et al.*, 2016; Olspert *et al.*, 2015; Rodamilans *et al.*, 2015). The PPV CP is *O*-GlcNAcylated by the OGT SEC (Chen *et al.*, 2005; Fernández-Fernández *et al.*, 2002). Seven Thr residues and one Ser that are modified by *O*-GlcNAcylation or influence the modification of other residues have been identified in the N-terminal region of PPV CP (Kim *et al.*, 2011; Pérez *et al.*, 2006, 2013; Scott *et al.*, 2006). Although *O*-GlcNAcylation of PPV CP is not essential for virus viability, it enhances viral infection (Chen *et al.*, 2005; Pérez *et al.*, 2013). PPV CP is also phosphorylated (Chen *et al.*, 2005; Fernández-Fernández *et al.*, 2002; Šubr *et al.*, 2007). A single amino acid mutation at the PPV CP N-terminus alters the protein phosphorylation status, suggesting that phosphorylated residues also lie in this region (Šubr *et al.*, 2010). The CP of another potyvirus, *Potato virus A* (PVA), is also phosphorylated, although the principal phosphorylation site identified is a Thr residue at the C-terminal end of the protein core region (Ivanov *et al.*, 2001, 2003; Lõhmus *et al.*, 2017).

Here, we used phosphopeptide analysis by tandem mass spectrometry (MS/MS) to identify the main phosphorylated residues in PPV CP. We used an iTRAQ (isobaric tags for relative and absolute quantitation) approach to assess possible crosstalk between phosphorylation and *O*-GlcNAcylation in PPV virions infecting wild-type and SEC-deficient *Nicotiana benthamiana* plants. To evaluate the relevance of CP phosphorylation for PPV infection, we also analysed infection by PPV mutants in which phosphorylation target sites were replaced by alanine (Ala) or by the phosphorylation mimic aspartic acid (Asp).

RESULTS

PPV CP is prone to phosphorylation at four Ser residues in the N-terminus and at the beginning of the core region that do not coincide with *O*-GlcNAcylated residues

Previous matrix-assisted laser desorption/ionization-time of flight (MALDI-TOF) analysis of purified PPV virions detected at least one phosphorylated residue in the tryptic peptide [1–39] in the N-terminal region of the viral CP (Chen *et al.*, 2005). To identify the number and specific location of putative modified sites, mass spectrometry approaches were used to map the phosphorylation sites in PPV virions purified from infected plants. Samples were digested with Lys-C and trypsin proteases, followed by phospho-enrichment before MS/MS; precursor peptide ions were selected on the basis of the mass-to-charge ratio (*m*/*z*) and fragmented to generate their corresponding mass spectra. Computer algorithms allowed peptide identification by matching experimental data with theoretical spectra derived from a homebuilt database that includes PPV CP. Signals corresponding to putative phosphorylated peptides were detected in the mass spectra. Two ESI (electrospray ionization)-based MS/MS systems, ion trap alternating electron-transfer dissociation/collision-induced dissociation (ETD/CID) fragmentation and high-resolution TripleTOF, unequivocally mapped four phosphorylation-prone Ser residues at positions 25, 81, 101 and 118 (Fig. 1; Table S1 and Fig. S1, see Supporting Information).

Phosphorylation at Ser residues 25, 81, 101 and 118 takes place alongside the previously described *O*-GlcNAcylation, which also modifies the N-terminal part of PPV CP at Thr residues 19, 24, 41, 50, 53, 54/58 and Ser-65 (Kim *et al.*, 2011; Pérez *et al.*, 2013). Residues susceptible to phosphorylation differ from those that can be *O*-GlcNAcylated (Fig. 1). As a result of the protease digestion, coexistence with *O*-GlcNAcylated residues on the same peptide was only possible for phosphoserines pSer-25 and pSer-81 (Fig. 1B); indeed, peptide [1–39] was detected as

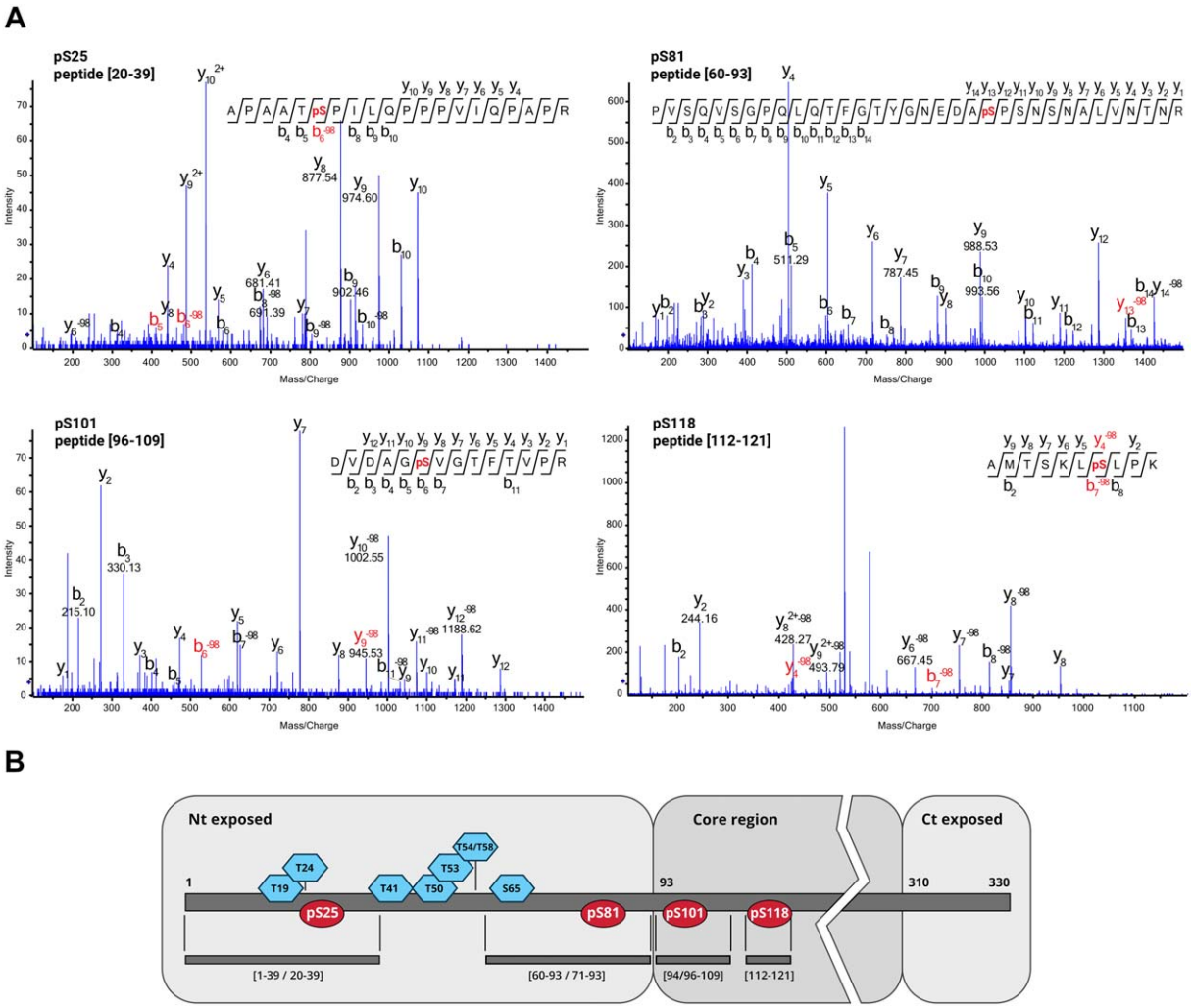

Fig. 1 Location of *Plum pox virus* (PPV) capsid protein (CP) phosphorylated residues. (A) Collision-induced dissociation-tandem mass spectrometry (CID-MS/MS) spectra corresponding to phosphorylated PPV CP peptides. (B) Scheme of PPV CP and its post-translational modifications (PTMs). Distribution of phosphorylated residues (red ellipses) and previously mapped *O*-GlcNAcylated amino acids (blue hexagons; Pérez *et al.*, 2013). Trypsin/Lys-C peptides in which the PTMs were identified are specified beneath the PPV CP map. Putative surface-exposed N- and C-terminal domains, as well as the protein core region, are shown on grey backgrounds. PPV CP domains are defined on the basis of predictions for other potyviral CPs (Baratova *et al.*, 2001, 2004; Ivanov *et al.*, 2003). Nt, N-terminus; Ct, C-terminus.

simultaneously phosphorylated at Ser-25 and *O*-GlcNAcylated at Thr-24 (Table S1). *O*-GlcNAc and *O*-phosphate groups thus do not compete for the same sites in PPV CP.

SEC down-regulation has a moderate effect on PPV CP phosphorylation

To determine how *O*-GlcNAcylation affects PPV CP phosphorylation in the context of active viral infection, we used SEC-b2 transgenic *N. benthamiana* plants in which *SEC* gene expression was down-regulated by RNA interference (RNAi) (Pérez, 2014). Virions purified from PPV-infected SEC-b2 plants were subjected to *O*-GlcNAc-specific immunodetection and MALDI-TOF analysis. Negligible *O*-GlcNAc-specific immunoreaction was detected, and *O*-GlcNAcylated tryptic peptide signals were greatly reduced in the MALDI spectra of these virions compared with controls (Fig. 2). Both tests showed that the *O*-GlcNAcylation level of PPV CP was very low in the SEC-deficient plants, consistent with a pronounced reduction in SEC activity.

For a quantitative view of PPV CP phosphorylation and *O*-GlcNAcylation in wild-type and SEC-deficient plants, we examined PPV virions purified from both plant types by an iTRAQ procedure coupled to immobilized metal affinity chromatography (IMAC) enrichment of phosphopeptides. For data analysis, we used the signal intensity values for peptides identified with a confidence interval >95% ($P < 0.05$) and a score value of >40, from two biological replicates per condition.

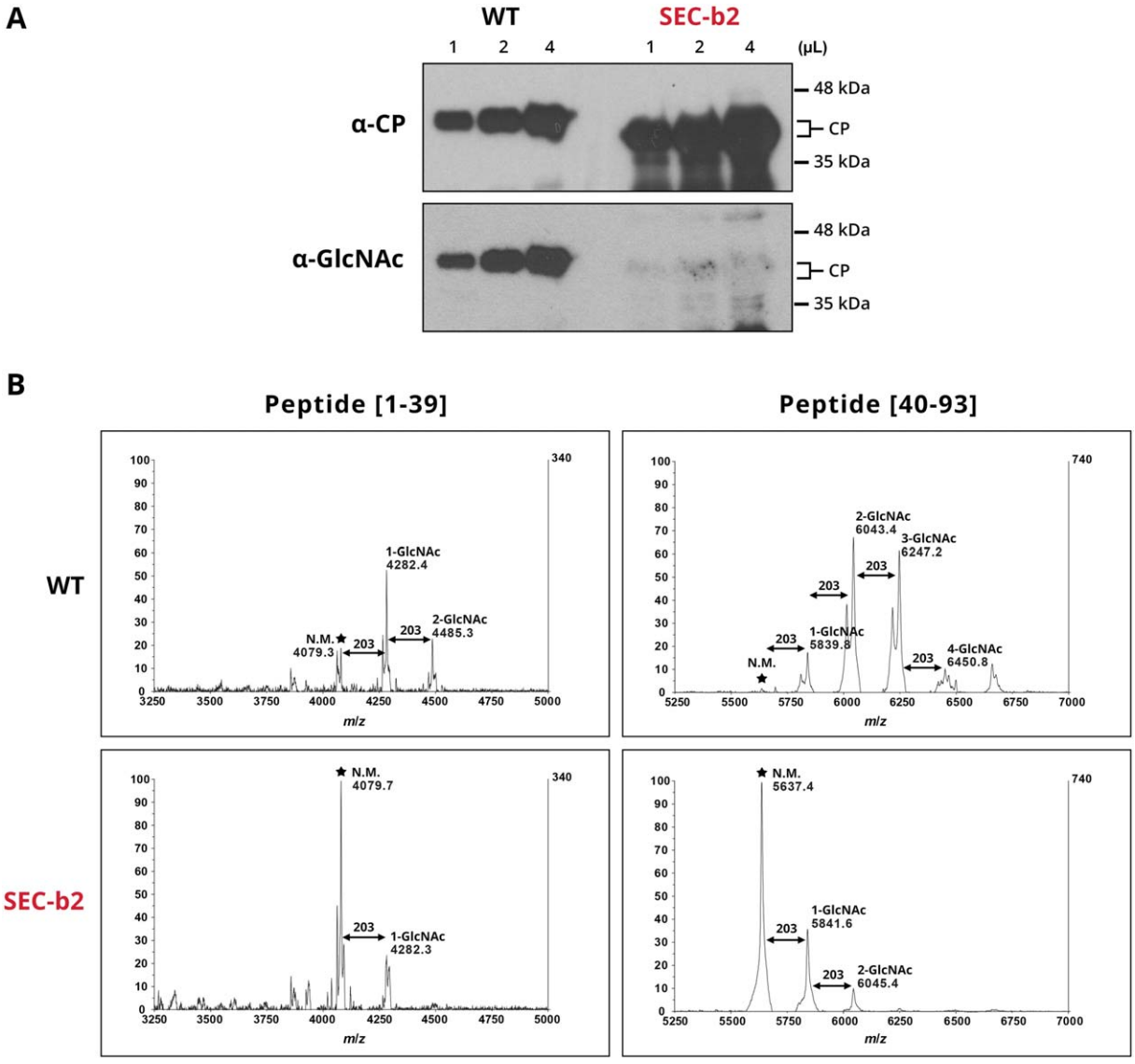

Fig. 2 *O*-GlcNAcylation of virions purified from wild-type (WT) and SECRET AGENT (SEC)-deficient (SEC-b2) *Nicotiana benthamiana* plants. (A) Similar amounts of *Plum pox virus* (PPV) virions purified from WT and SEC-b2 plants were subjected to immunoblot analysis. The same membrane was probed consecutively with PPV capsid protein (CP)- and *O*-GlcNAc-specific antibodies. Molecular mass ladder, right. (B) Matrix-assisted laser desorption/ionization-time of flight (MALDI-TOF) spectra covering the region corresponding to peptides from 1 to 39 and 40 to 93 amino acids. Mass/charge ratios (*m/z*) assigned to relevant peaks, as well as the predicted number of *O*-GlcNAc residues that modify each peptide species, are shown in each case. Stars mark the unmodified parental peaks corresponding to tryptic peptides [1–39] and [40–93].

In accordance with the MALDI-TOF analysis (Fig. 2B), both non-glycosylated and mono- and di-*O*-GlcNAcylated species of peptides [1–39] and [15–39] had high-intensity values in wild-type plant samples. In contrast, mono- and poly-*O*-GlcNAcylated peptide forms [40–59] and, especially, [40–93] showed low intensity, even in wild-type plant samples (Table S2, see Supporting Information). These data suggest that recovery efficiency throughout iTRAQ handling can differ for distinct peptide species. Although relative amounts of the same peptide in different protein samples can be compared reliably, comparison of intensity ratios for distinct peptides should be interpreted with caution, as peptide-dependent physicochemical properties can lead to different response intensity.

As predicted, comparison of glycosylation levels of wild-type and SEC-b2-derived peptides showed much lower abundance of glycosylated forms in SEC-deficient conditions. The ratio of intensity values for *O*-GlcNAcylated peptides [1–39] and [15–39] to the sum of intensity values of all species of each peptide was more

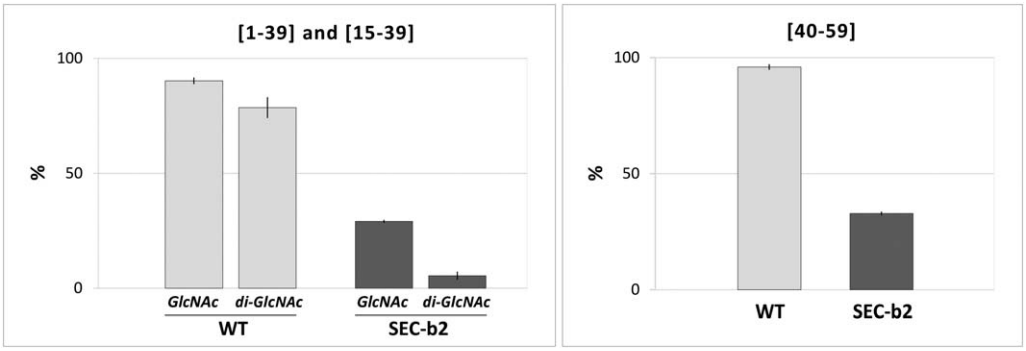

		WT (1)	WT (2)	WT average	SEC-b2 (1)	SEC-b2 (2)	SEC-b2 average
[1-39] [15-39]	*Overall O-GlcNAc*	88.61	92.01	**90.29**	30.06	28.20	**29.12**
	di-O-GlcNAc	74.36	83.14	**78.63**	8.59	3.40	**5.40**
[40-59]	*Overall O-GlcNAc*	94.42	97.46	**95.93**	31.71	33.96	**32.82**

Fig. 3 Reduction of *Plum pox virus* (PPV) capsid protein (CP) *O*-GlcNAcylation in SECRET AGENT (SEC)-deficient plants. Percentages were calculated as the sum of iTRAQ (isobaric tags for relative and absolute quantitation) intensity values for the *O*-GlcNAcylated species (overall *O*-GlcNAc) or di-*O*-GlcNAcylated species (di-*O*-GlcNAc), each divided by the sum of the intensity values of all species of the specified peptides. The table shows values for each biological replica of PPV virions, purified from wild-type (WT) and SEC-b2 *Nicotiana benthamiana* plants, and corresponding averages. Mean values are plotted in the histograms (top) and range values are shown as vertical lines.

than threefold lower in SEC-b2 relative to wild-type samples (29.1% versus 90.3%) (Fig. 3). *O*-GlcNAcylation differences were even more evident for di-*O*-GlcNAcylated peptide species [1–39] and [15–39], which were approximately 15 times less abundant in SEC-deficient than in wild-type plants (5.4% versus 78.6%) (Fig. 3). Although the recovery of peptide species, including *O*-GlcNAc targets downstream of residue 40 (Thr-41, Thr-50, Thr-53, Thr-54/58, Ser-65), was poor in the iTRAQ assay, we detected a notable decrease in *O*-GlcNAcylation for peptide [40–59] in SEC-deficient relative to wild-type samples (32.8% versus 95.9%) (Fig. 3).

We detected phosphorylation at Ser-25, alone or in combination with *O*-GlcNAcylation of Thr-24 or of Thr-24 and Thr-19, in peptides [1–39] and [15–39] (Table S2). This indicates that both PTMs are compatible and can affect the PPV CP N-terminus concomitantly. Although iTRAQ intensities of different peptide species in the same sample must be compared with care, the finding in all cases that the ratio of phosphorylated to non-phosphorylated species was notably lower for *O*-GlcNAcylated (0.04–0.06) than for non-glycosylated (0.14–0.11) peptides suggests some cross-interference between these PTMs (Fig. 4). This idea was supported by the data obtained when we compared Ser-25 phosphorylation levels; the ratio of intensity values for phosphorylated Ser-25 to all potential species of the [1–39] and [15–39] peptides was markedly lower in wild-type than in SEC-deficient plant virions (4.4% versus 8.8%) (Fig. 4).

Phosphorylation at Ser-81 was detected in peptides [40–93], [60–93] and [60–95] in wild-type and SEC-deficient plants (Table S2). The phosphorylation levels, estimated as the ratio of the sum of intensity values for phosphorylated Ser-81 in these three peptides to that for all peptide species, were similar in wild-type and SEC-deficient samples (Fig. S2, see Supporting Information). The fact that glycosylated forms of these peptides (phosphorylated or non-phosphorylated) were rarely detected in this iTRAQ experiment nonetheless calls for caution when interpreting these data.

The phosphorylation target at Ser-101 is included in peptides [94–109] and [96–109], which do not contain residues predicted to be *O*-GlcNAcylated. We detected phosphorylated forms of these peptides, but with much lower intensity than that of unmodified species, which was similar in wild-type and SEC-deficient plants (Fig. S2).

Peptide [112–121] is the only peptide bearing Ser-118 which was identified with certainty in iTRAQ analysis. The only species found was phosphorylated, which suggests that Ser-118 is always phosphorylated in CP assembled in PPV virions. This peptide nonetheless contains an internal lysine (Lys) (K116 in Fig. S3, see Supporting Information) and is thus a partially digested product of Lys-C/trypsin treatment. A possible explanation for this incomplete proteolysis is that pSer-118 hampers enzyme cleavage at Lys-116. We cannot rule out the possibility that the fully processed peptide [117–121] was generated and not detected, as it is too small to generate a number of fragment ions sufficient for confident identity assignment by MS/MS. In any case, the similarity of intensity

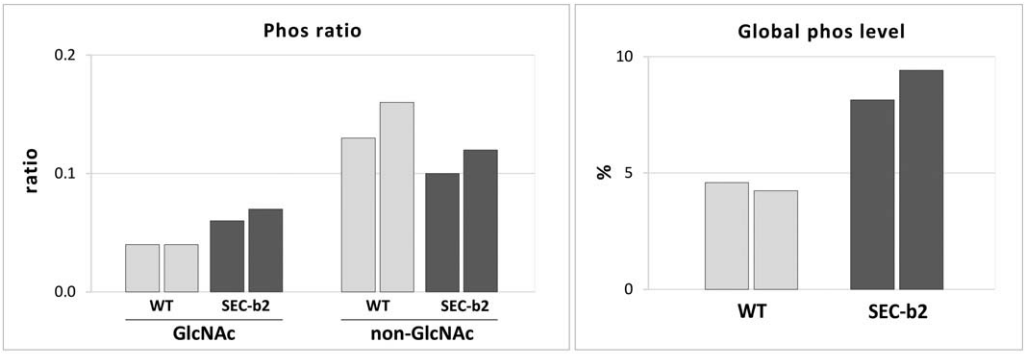

[1-39] and [15-39]		WT (1)	WT (2)	WT average	SEC-b2 (1)	SEC-b2 (2)	SEC-b2 average
Specific Phos Ratio	GlcNAc	**0.04**	**0.04**	0.04	**0.06**	**0.07**	0.06
	non-GlcNAc	**0.13**	**0.16**	0.14	**0.10**	**0.12**	0.11
Global Phos level (%)		**4.58**	**4.23**	4.40	**8.14**	**9.41**	8.75

Fig. 4 Effect of decreased *O*-GlcNAcylation on the phosphorylation level of *Plum pox virus* (PPV) capsid protein (CP) at Ser-25. The table shows ratios of iTRAQ (isobaric tags for relative and absolute quantitation) intensity values of phosphorylated versus non-phosphorylated species for peptides including Ser-25 ([1–39] and [15–39]). Species that are also *O*-GlcNAcylated (GlcNAc) and non-glycosylated (non-GlcNAc) are compared. The table also compares percentages of intensity values of phosphorylated species with all peptide species [1–39] and [15–39]. Values for each biological replica of PPV virions purified from wild-type (WT) and SEC-b2 *Nicotiana benthamiana* plants, and corresponding averages, are shown. Individual values are plotted in histograms (top).

of the phosphorylated peptide species [112–121] in the wild-type and SEC-deficient samples (Table S2) suggests that Ser-118 phosphorylation is largely independent of protein *O*-GlcNAcylation.

In order to confirm the effect of *O*-GlcNAcylation on the level of phosphorylation in Ser-25 by an additional technique, we conducted a label-free quantification assay comparing the abundance of the phosphorylated and/or *O*-GlcNAcylated forms of the peptide [1–39] in PPV virions purified from wild-type and SEC-deficient SEC-b2 plants (Table S3, see Supporting Information). The results confirmed the low-level *O*-GlcNAcylation of the [1–39] peptide in SEC-b2 plants (8.3% versus 75.0% in the wild-type plants). More importantly, the level of phosphorylation of the [1–39] peptide was increased more than two-fold in the PPV virions purified from SEC-deficient plants compared with those from wild-type plants (5.5% versus 2.3%).

All of these data confirm that *O*-GlcNAcylation and phosphorylation can coexist in the same PPV CP molecule, but suggest that the effect of the *O*-GlcNAcylation level on phosphorylation varies for different target sites.

Relevance of CP phosphorylation for PPV infection

To determine the influence of the phosphorylation state of the CP N-terminus in PPV infection, the four phosphorylatable Ser residues mapped, Ser-25, Ser-81, Ser-101 and Ser-118, were replaced by Ala residues (4SA) to prevent phosphorylation, or by Asp (4SD) to emulate a constitutive phosphorylated state. These mutations were engineered into the full-length cDNA clones pICPPV-NK-lGFP (h-4SA, h-4SD) and pICPPV-5′BD-GFP (sf-4SA, sf-4SD), suitable for the infection of herbaceous plants and *Prunus* seedlings, respectively (Fig. S3).

Effect of abolishing or emulating CP phosphorylation on PPV infection in Nicotiana benthamiana

N. benthamiana plants were initially inoculated by DNA bombardment with h-4SA and h-4SD mutants, as well as with the h-WT virus. We detected systemic infection in a variable number of plants bombarded with h-WT (5/10), h-4SA (8/10) and h-4SD (2/9). In addition to its lower infectivity, the h-4SD mutant accumulated in smaller amounts than the h-4SA and h-WT viruses (Fig. S4, see Supporting Information). Immunocapture-reverse transcription-polymerase chain reaction (IC-RT-PCR) amplification and sequencing of a cDNA fragment from the CP coding region confirmed 4SA and 4SD mutation stability.

New plants were inoculated by hand-rubbing with extracts of systemically infected leaves from previously bombarded plants. The h-4SD inoculum was eight times more concentrated than h-4SA and h-WT inocula to compensate for differences in viral accumulation in the first plants infected. Although h-4SA showed no differences compared with the h-WT virus, systemic symptoms in h-4SD-infected plants were delayed and milder than those of plants infected with h-4SA or h-WT. In contrast with the results of

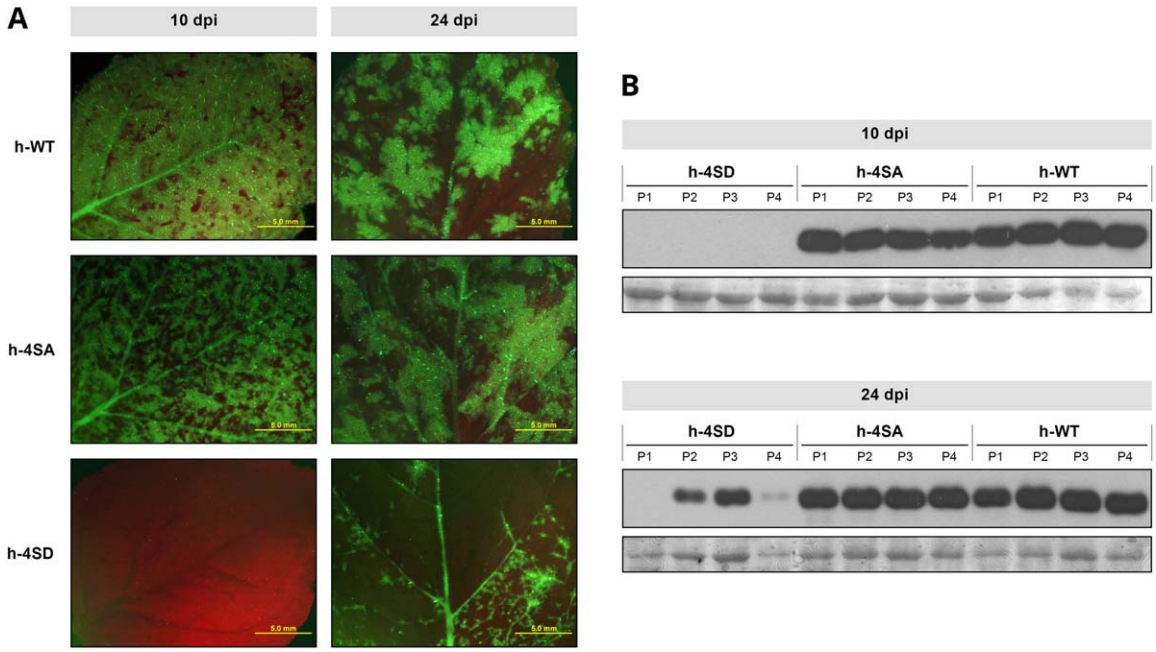

Fig. 5 Infection of *Nicotiana benthamiana* by wild-type *Plum pox virus* (PPV) (h-WT) and PPV mutants bearing changes that prevent (h-4SA) or mimic (h-4SD) capsid protein (CP) phosphorylation, at serine residues 25, 81, 101 and 118. Plants were inoculated by hand-rubbing with leaf extracts of previously infected *N. benthamiana* plants. (A) Images of upper uninoculated leaves of plants infected with the indicated viruses, at 10 or 24 days post-inoculation (dpi), under an epifluorescence microscope. Bars, 5 mm. (B) PPV CP-specific immunoblot analysis of extracts from upper uninoculated leaves from four individual plants infected with viruses as indicated. Samples were collected at 10 and 24 dpi. Blots stained with Ponceau red showing the ribulose-1,5-bisphosphate carboxylase/oxygenase (RuBisCO) protein are included as loading controls.

gene-gun inoculation, there were no large differences in viral accumulation in plants infected with h-WT, h-4SA or h-4SD (not shown). Sequence analysis of viral progeny of several h-4SA- and h-4SD-infected plants showed conservation of the initial mutations in all cases. In two of the four 4SD-infected plants, however, new mutations emerged in positions distant from the initial mutation sites, Y266F in one case and T254K in another.

To further characterize the 4SD phenotype, we used leaf extract from an h-4SD-infected plant whose viral progeny conserved the initial CP sequence as inoculum for a new infection round. In this experiment, all inoculated plants were infected. Systemically infected leaves were analysed at different days post-inoculation (dpi). At 10 dpi, plants infected with h-WT and h-4SA showed clear symptoms, abundant green fluorescent protein (GFP) expression and similar levels of virus accumulation as assessed by immunoblot analysis (Fig. 5). At the same time point, plants inoculated with h-4SD showed no symptoms, GFP expression or virus accumulation (Fig. 5). By 15 dpi, mild disease symptoms began to appear in h-4SD-inoculated plants; GFP expression and viral CP accumulation were clear, but quite variable, at 24 dpi, and remained lower than in h-4SA- and h-WT-infected plants (Fig. 5). We found no changes in the CP sequence of four 4SD-infected plants analysed.

These results show that the lack of phosphorylation in PPV CP does not alter noticeably viral infection, but that mimicking of phosphorylation at phosphorylatable sites delays infection and fosters the selection of potentially compensatory second mutations.

Effect of abolishing or emulating CP phosphorylation in PPV infection on Nicotiana clevelandii, Chenopodium foetidum and Prunus persica

To search for any host-specific effects that abolishing or emulating CP phosphorylation could have on PPV infection, we challenged another herbaceous systemic PPV host, *Nicotiana clevelandii*, as well as the herbaceous local host *Chenopodium foetidum* and the natural woody host *Prunus persica* with phosphorylation-related PPV mutants.

N. clevelandii plants were inoculated by hand-rubbing with leaf extracts of *N. benthamiana* plants infected with h-4SA, h-4SD or h-WT. Symptoms in plants infected with h-4SA or h-WT were conspicuous by 10 dpi, when comparable high levels of virus accumulation were detected in these plants by immunoblot analysis. As for *N. benthamiana*, neither symptoms nor h-4SD virus accumulation was observed at 10 dpi, although the accumulation of the mutant was easily detected in this host at 24 dpi (Fig. S5A,B, see Supporting Information).

Table 1 Infectivity in *Prunus persica* of wild-type *Plum pox virus* (PPV) (sf-WT) and PPV mutants with modifications that prevent (sf-4SA) or mimic (sf-4SD and sf-S118D) capsid protein (CP) phosphorylation.

Inoculum	Assay No. 1*	Assay No. 2*
sf-WT	5/5	5/5
sf-4SA	4/5	–
sf-4SD	0/5	0/9
sf-S118D	–	5/5

*Infected/inoculated plants.

In *C. foetidum*, the h-4SA mutant caused necrotic local lesions similar to those of the wild-type virus. The h-4SD mutant was also able to infect *C. foetidum*, although the lesions were far less numerous and milder, with later onset, than those promoted by h-WT or h-4SA (Fig. S5C).

To assess the effect of disturbing CP phosphorylation on PPV infection of a natural woody host, we inoculated *P. persica* seedlings by bombardment with multiple mutants sf-4SA and sf-4SD and the wild-type virus sf-WT. As in herbaceous hosts, the sf-4SA mutant showed infectivity, pathogenicity and accumulation similar to that for the wild-type virus (Table 1 and Fig. 6). No infection symptoms were detected in any of the seedlings inoculated with the sf-4SD mutant. Moreover, neither GFP fluorescence under UV irradiation, nor virus accumulation as assessed by immunoblot analysis, was detected in the 4SD-inoculated peach seedlings (Fig. 6).

These results indicate that constitutive phosphomimicking in CP affected PPV infection in all plant species analysed, with a greater effect in the natural host *P. persica*.

Effect on PPV fitness of mutations that prevent CP phosphorylation

To search for possible subtle effects on viral infection efficiency caused by the prevention of PPV CP phosphorylation, we performed competition experiments of the mutant h-4SA and wild-type virus in mixed infections in *N. benthamiana* and *N. clevelandii*. Mixtures of extracts of *N. benthamiana* plants infected with h-4SA and h-WT, in which the mutant virus was over-represented (either 1 : 0.6 or 1 : 0.4), were inoculated in *N. benthamiana* and *N. clevelandii* plants ($n = 4$ plants each, in total). At 14 dpi, RT-PCR amplification and sequencing of a cDNA fragment from the CP coding region detected only h-4SA in the four *N. benthamiana* plants and in one *N. clevelandii* plant (Fig 7; Fig. S6, see Supporting Information), which confirmed that competitiveness of the mutant is not much lower than that of the wild-type virus. Despite its lesser amount in the inoculum, the wild-type virus was detected in three *N. clevelandii* plants, and was exclusive in two of these (Fig 7, Fig. S6), which may suggest slightly lower h-4SA mutant fitness than that of the wild-type virus.

To test this possibility, we inoculated an extract from an *N. clevelandii* plant in which h-4SA and h-WT coexisted at apparently similar levels (plant P2 in Fig. 7) into four *N. benthamiana* and three *N. clevelandii* plants; the viral populations of these plants were tested by RT-PCR and sequencing. In one *N. benthamiana* plant, the wild-type virus outcompeted the h-4SA mutant and, in the remainder, the mutant population appeared to be much less abundant than in the inoculum (Fig 7, Fig. S6).

The results from the competition experiments thus suggest that, although mutations that prevent CP phosphorylation do not cause severe effects in PPV infection, they can slightly reduce viral fitness in *Nicotiana* species.

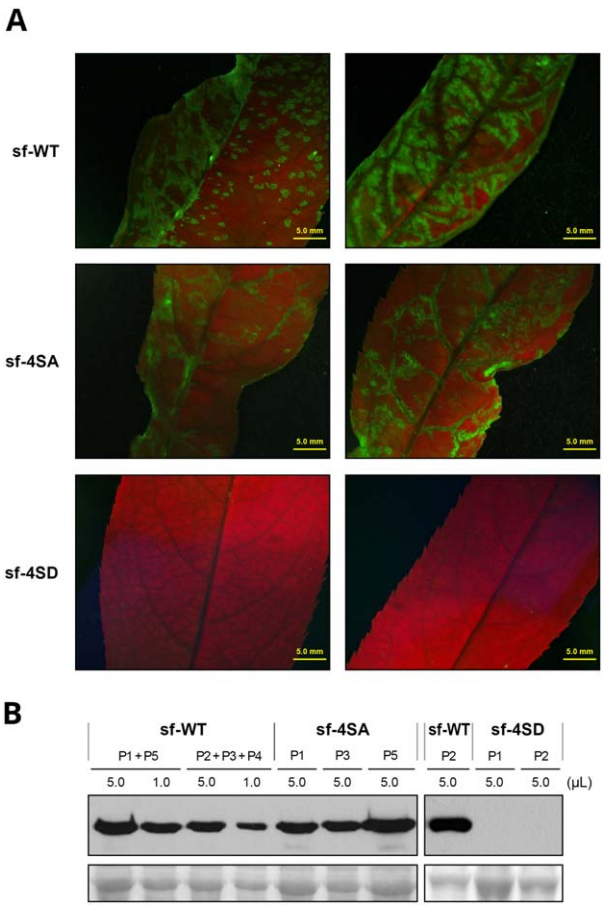

Fig. 6 Infection in *Prunus persica* by wild-type *Plum pox virus* (PPV) (sf-WT) and PPV mutants carrying changes that prevent (sf-4SA) or mimic (sf-4SD) capsid protein (CP) phosphorylation at serine residues 25, 81, 101 and 118. *P. persica* seedlings were inoculated by bombardment with viral cDNA. (A) Images of upper uninoculated leaves of plants infected with the indicated viruses, at 21 days post-inoculation (dpi), under an epifluorescence microscope. Bar, 5 mm. (B) PPV CP-specific immunoblot analysis of extracts from upper uninoculated leaves for individual or pooled plants, collected at 21 dpi. Viruses used as inocula and volume of extract loaded are indicated. Blots stained with Ponceau red showing the ribulose-1,5-bisphosphate carboxylase/oxygenase (RuBisCO) protein are included as loading control.

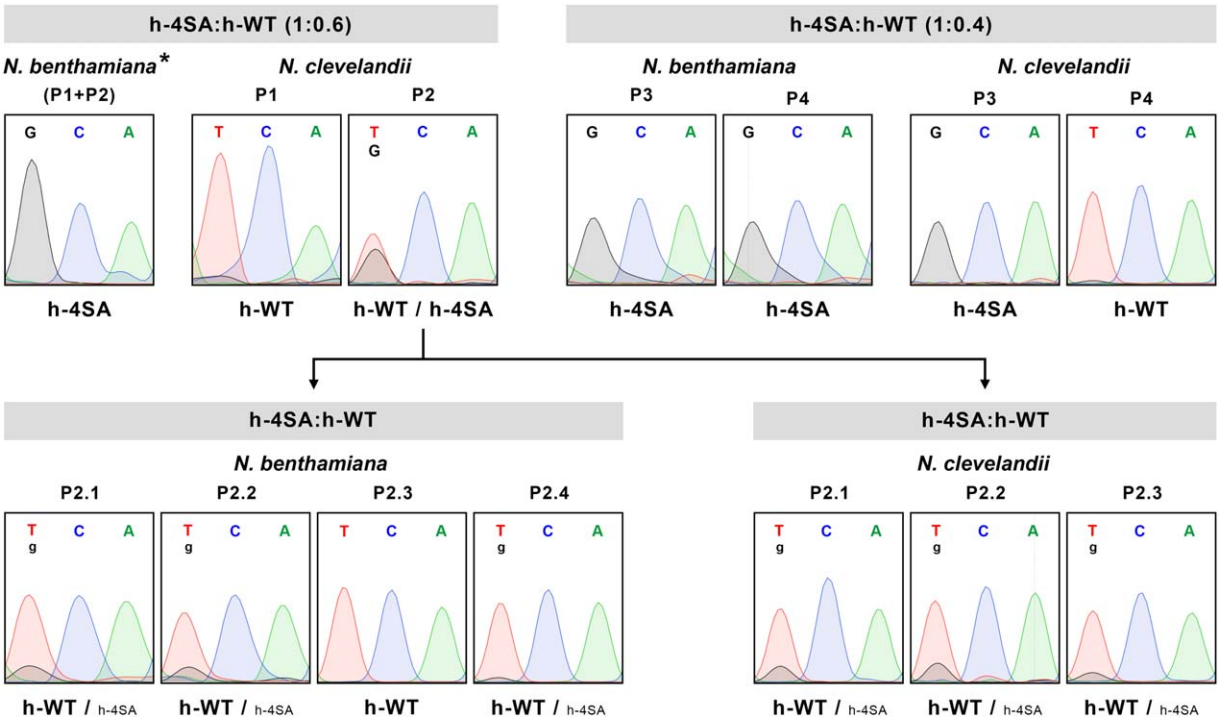

Fig. 7 Sequence analysis of viral progeny from mixed infections with wild-type *Plum pox virus* (PPV) (h-WT) and a PPV mutant carrying changes that prevent capsid protein (CP) phosphorylation at serine residues 25, 81, 101 and 118 (h-4SA). Mixtures of extracts of *Nicotiana benthamiana* plants infected with h-4SA and h-WT, combined at the indicated ratios, were used to inoculate *N. benthamiana* and *Nicotiana clevelandii* plants. Viruses in infected plants were identified by reverse transcription-polymerase chain reaction (RT-PCR) and sequencing of a cDNA fragment covering the CP coding region. An extract from an *N. clevelandii* plant in which h-WT and h-4SA accumulated at similar levels (P2) was used to inoculate new *N. benthamiana* and *N. clevelandii* plants, whose viral progeny were assessed as above. Images show the region of sequencing chromatograms corresponding to the triplet encoding CP residue 81 (TCA in h-WT or GCA in h-4SA). The viruses identified are indicated beneath the chromatograms; smaller letters indicate lower accumulation. Individual plants (P1–P4 and P2.1–P2.4) were analysed except for the pool of *N. benthamiana* plants (P1 + P2) indicated by an asterisk (*).

Effect of mimicking phosphorylation in PPV CP residue 118 on viral infection

Mutation S118D in the h-4SD mutant is unstable

The detection of the Y266F and T254K substitutions in two h-4SD-infected plants suggests that the slower infection rate in these plants could promote the selection of compensatory mutations that mitigate the negative effects of phosphorylation mimicking.

To increase the chances of h-4SD mutant adaptation, two sets of 37 plants were inoculated by leaf-rubbing with leaf extracts from two plants infected with h-4SD whose viral progeny showed no secondary mutations. All inoculated plants were infected, although two distinct phenotypes were observed. By 25 dpi, 35 plants of one set and two of the other showed the chlorotic mottling typical of PPV infection, whereas the remaining plants showed only delayed, mild symptoms. RT-PCR amplification and sequencing of appropriate cDNA fragments confirmed an intact CP sequence in the viral progeny of plants with the delayed mild phenotype. In contrast, we observed a G-to-A mutation that caused an Asp-to-asparagine (Asp-to-Asn) change in residue 118 in the subgroup with the accelerated severe phenotype ($n = 35$) in the first set of h-4SD-infected plants; in addition, we found a G-to-A mutation that caused an arginine-to-glutamine (Arg-to-Gln) substitution at CP residue 237 in the viral progeny of these plants (Fig. S7, see Supporting Information). An A-to-G mutation causing a change to glycine (Gly) was detected in the same residue 118 in the subgroup with early severe symptoms ($n = 2$) of the second set of plants (Fig. S7). Extracts of plants infected with intact h-4SD or with the Asn-118/Gln-237 or Gly-118 variants were used to inoculate a new batch of *N. benthamiana* plants, which reproduced the phenotype of the parental plants. No changes in the CP sequence relative to the inocula were detected in these infected plants.

Effect of S118D mutation is reinforced by additional phosphomimetic mutations

The D118 instability suggests that the h-4SD defects are mainly the result of the S118D mutation. To verify this possibility and to assess the relevance of phosphomimetic mutations in the remaining phosphorylatable residues, we constructed the single mutants h-S25D, h-S81D, h-S101D and h-S118D, and hand-inoculated them, as well as a control h-4SD mutant, in *N. benthamiana* by

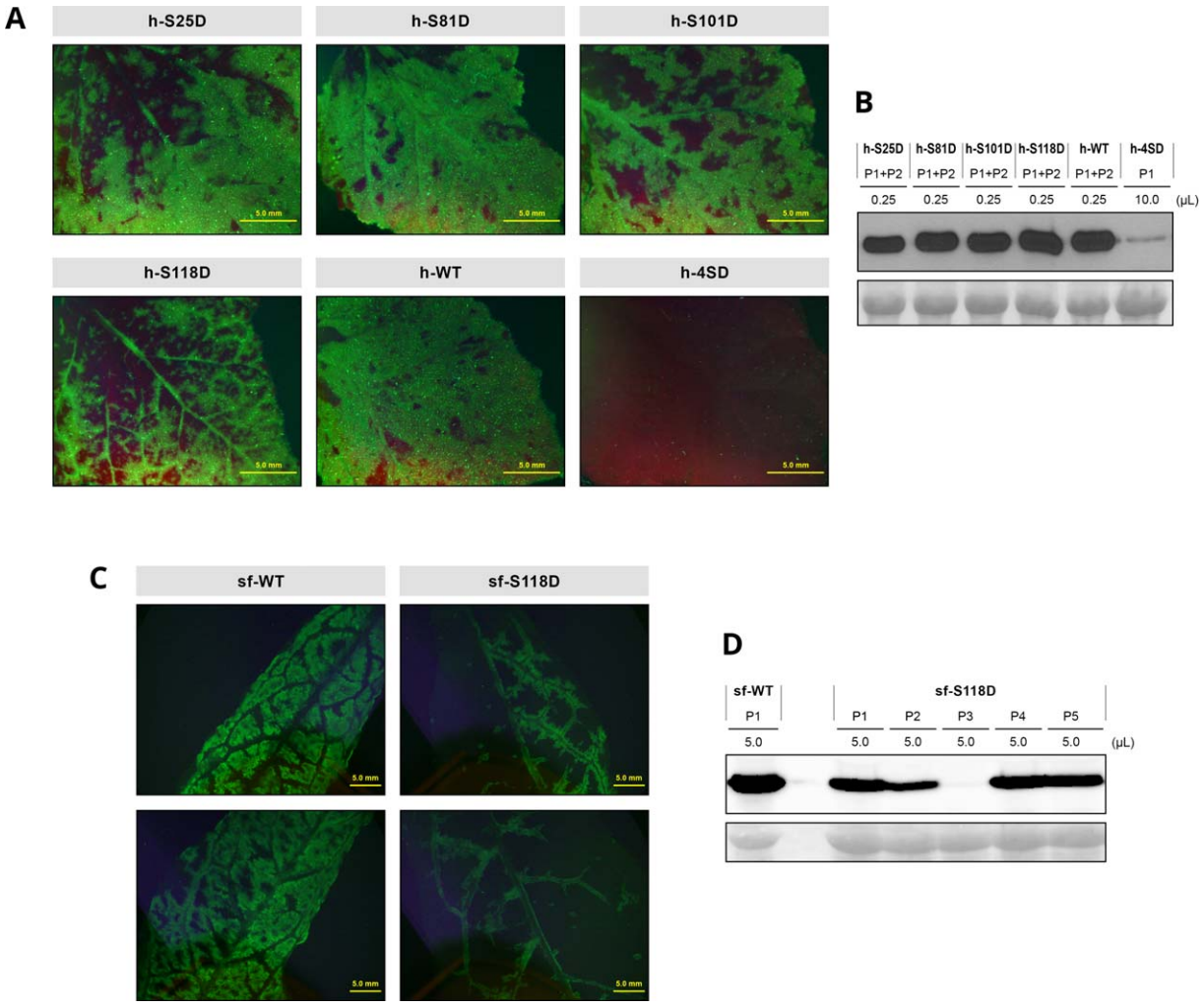

Fig. 8 Infection of *Nicotiana benthamiana* and *Prunus persica* plants by wild-type *Plum pox virus* (PPV) and PPV mutants bearing phosphorylation-mimicking mutations in the capsid protein (CP). Plants were inoculated by hand-rubbing (*N. benthamiana*) or bombardment (*P. persica*) with viral cDNA. (A, C) Images of upper uninoculated leaves of *N. benthamiana* (A) or *P. persica* (C) plants after infection with the indicated viruses, taken at 21 or 23 days post-inoculation (dpi), respectively, under an epifluorescence microscope. Bar, 5 mm. (B, D) PPV CP-specific immunoblot analysis of extracts from upper uninoculated leaves of *N. benthamiana* (B) or *P. persica* (D) individual or pooled plants, collected at 21 dpi (*N. benthamiana*) or 23 dpi (*P. persica*). Inoculated viruses and extract volumes loaded are indicated. Blots stained with Ponceau red showing the ribulose-1,5-bisphosphate carboxylase/oxygenase (RuBisCO) protein are included as loading control.

rubbing leaves with cDNA. The infectivity of all single mutants was similar to that of the wild-type virus (Table S4, see Supporting Information). The symptoms for the four single mutants were similar to those of the wild-type virus, although h-S118D-infected plants showed an apparent brief delay (not shown). Immunoblot analysis at 21 dpi, when h-4SD mutant accumulation was almost undetectable, showed similar accumulation of the h-S25D, h-S81D, h-S101D and h-S118D mutants, comparable with that of the wild-type virus (Fig. 8A,B). The initial Ser-to-Asp mutations were stable in the viral progeny of the two infected plants analysed for each virus. Although we detected a new P67S mutation in the viral progeny of one h-4SD-infected plant, no additional mutations were detected in the CP sequence of any single mutants. This suggests that the deleterious effect of mimicking phosphorylation in residue 118 is reinforced when phosphorylation is also mimicked in other phosphorylatable CP residues. However, the distinct effect of the S118D mutation was highlighted by the fact that a viral species with Asn in position 118 emerged when h-S118D progeny were inoculated into new plants. In contrast, h-S25D, h-S81D and h-S101D remained stable when passaged in the same conditions.

To further assess the relevance of the S118D phosphomimetic mutation, it was constructed in the pICPPV-5′BD-GFP backbone and the resulting sf-S118D mutant was inoculated in *P. persica* seedlings by particle bombardment, using the multiple mutant sf-4SD and the sf-WT virus as controls (Fig. S3). The inability of

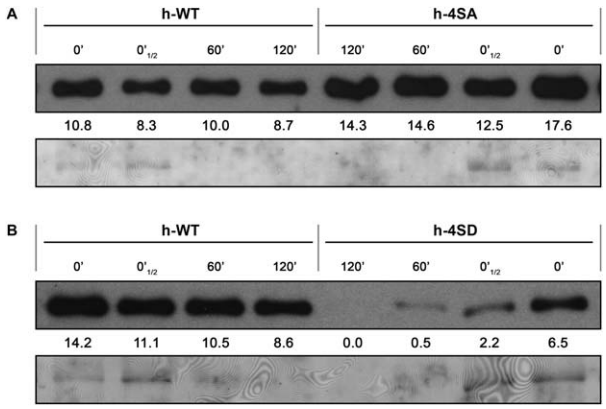

Fig. 9 Stability assay of *Plum pox virus* (PPV) capsid protein (CP), either wild-type (h-WT) or bearing phosphorylation-preventing (h-4SA) or phosphorylation-mimicking (h-4SD) mutations. Systemically infected tissue from *Nicotiana benthamiana* plants, inoculated by hand-rubbing with infected extract, was collected at 21 days post-inoculation (dpi). After verification by reverse transcription-polymerase chain reaction (RT-PCR) and sequencing that viral progeny did not hold unintended mutations, native extracts were prepared in phosphate buffer and CP accumulation was assessed by immunoblot analysis immediately after extraction (0′ and $0'_{1/2}$, in which a half amount of sample was loaded) or after incubation for the indicated times. The stabilities of h-4SA and h-4SD CPs are compared with that of the wild-type CP (h-WT) in (A) and (B), respectively. The intensity values of the CP bands were calculated with Quantity One 1-D software (Bio-Rad, USA) and are shown below each lane. Blots stained with Ponceau red showing the ribulose-1,5-bisphosphate carboxylase/oxygenase (RuBisCO) protein are included as loading control.

sf-4SD to infect peach seedlings was confirmed, whereas sf-S118D infectivity was similar to that of the wild-type virus (Table 1). Symptoms of the mutant appeared to be somewhat milder and its accumulation was slightly lower than that of the wild-type virus (Fig. 8C,D). RT-PCR analysis showed that the S118D mutation was stable in the peach viral progeny. These data further support the conclusion that phosphomimicry in several CP residues contributes collectively to disturb PPV infection.

Emulation of constitutive phosphorylation affects the in vitro stability of PPV CP

To determine whether the impairment of PPV infection caused by mutations emulating constitutive CP phosphorylation could be related to altered protein stability, the CPs of wild-type PPV and of the h-4SA and h-4SD mutants were subjected to an endogenous degradation assay. A time course analysis of CP accumulation was carried out in cell-free extracts prepared in native conditions from systemically infected leaves of *N. benthamiana* plants incubated at 25 °C. Wild-type and h-4SA CP were detected at a similar high level even after 2 h of incubation (Fig. 9A), which indicates that prevention of phosphorylation does not have a detrimental impact on CP stability. In contrast, a very small amount of the phosphomimicking h-4SD CP mutant remained intact after 2 h of incubation (Fig. 9B). This latter finding suggests that reduced protein stability could contribute to the deleterious effect of the emulation of constitutive phosphorylation on PPV infection.

DISCUSSION

Phosphorylation and *O*-GlcNAcylation are two PTMs that affect the same protein residues, Thr and Ser, and play crucial regulatory roles in a large number of biological processes (Hart *et al.*, 2011). Dynamic interactions between these PTMs have been studied extensively for mammalian proteins (Comer and Hart, 2000; Hart *et al.*, 2011; Slawson and Hart, 2003; Zeidan and Hart, 2010). Although some plant proteins are also modified by both phosphorylation and *O*-GlcNAcylation (Chen *et al.*, 2005; Taoka *et al.*, 2007; Xing *et al.*, 2009; Xu *et al.*, 2017; Zentella *et al.*, 2016), the interplay of these PTMs in plants is largely unknown. Although several proteins of plant viruses are known to be phosphorylated (Champagne *et al.*, 2007; Hoover *et al.*, 2016; Hu *et al.*, 2015; Hung *et al.*, 2014; Ivanov *et al.*, 2003; Jakubiec *et al.*, 2006; Lee and Lucas, 2001; Link *et al.*, 2011; Módena *et al.*, 2008; Puustinen *et al.*, 2002; Samuilova *et al.*, 2013; Shapka *et al.*, 2005; Zhao *et al.*, 2015), there is evidence that the CP of the potyvirus PPV is both phosphorylated and *O*-GlcNAcylated (Chen *et al.*, 2005; Fernández-Fernández *et al.*, 2002; Šubr *et al.*, 2007); this makes this protein an excellent model to study how phosphorylation and *O*-GlcNAcylation jointly regulate protein activity in plant cells and to define the roles of these PTMs in viral infections.

Our results identify four phosphorylation sites in the N-terminal half of PPV CP, which do not overlap with known *O*-GlcNAcylation targets. We show that, although phosphorylation at these residues is not essential for virus viability, phosphorylation mimicking in phosphoacceptor residues is deleterious for viral infection. Some mammalian proteins adhere to a 'yin–yang' model in which phosphorylation and *O*-GlcNAcylation compete for the same target sites (Wells *et al.*, 2001). Taoka *et al.* (2007) found evidence that the same Ser residue of the *Cucurbita maxima* protein Cm-PP16-1 was targeted by both PTMs, which suggests that

the 'yin–yang' model may apply to plant proteins, but the concurrence of phosphorylation and *O*-GlcNAcylation, although rare, has been observed in some Arabidopsis proteins identified in the high-throughput proteomic analysis conducted by Xu *et al.* (2017). This is also the case for the PPV CP. The previously identified *O*-GlcNAcylated targets map to the region between residues 19 and 65 (Pérez *et al.*, 2013), and we found that none were alternatively phosphorylated (Fig. 1). One of the phosphorylated residues, Ser-25, is located in this region beside the *O*-GlcNAcylatable Thr-24 (Fig. 1). We readily detected peptide [1–39] species concurrently phosphorylated at Ser-25 and *O*-GlcNAcylated at Thr-24 (Tables S1 and S2), which indicates that phosphorylation and *O*-GlcNAcylation do not competitively block each other at these sites. Nonetheless, this does not imply that phosphorylation and *O*-GlcNAcylation of PPV CP are completely independent. The enhanced phosphorylation at Ser-25 in *O*-GlcNAcylation-deficient transgenic plants indicates crosstalk between these PTMs.

Another phosphorylated residue, Ser-81, is found further from the *O*-GlcNAcylated region, but is within the N-terminal protrusion of the protein, whereas the other two phosphorylation targets identified here are located at the beginning of the core region (Fig. 1). We found no evidence that phosphorylation at these three sites is influenced by the *O*-GlcNAcylation state of the protein (Fig. S2 and Table S2). Our results do not allow us to predict whether the distinct *O*-GlcNAcylation dependence reflects metabolic or functional differences.

In silico analysis showed no clear similarities in the sequences surrounding the four phosphorylation sites reported here. Of these, only Ser-118 was fully conserved in all PPV strains (Fig. S8, see Supporting Information) and none was highly conserved amongst potyviral CPs (not shown), which suggests that phosphorylation at precise positions of the CP N-terminal half is not necessary for basal functions of potyviral infection. In accordance with this assumption, a multiple mutant in which the four phosphoacceptor Ser residues of this region were replaced by Ala residues infected both herbaceous and woody hosts efficiently (Fig. 5, Fig. 6; Fig. S4, Fig. S5). In contrast, Ser-to-Asp mutations that mimicked phosphorylation at these sites appeared to be deleterious for viral infection, especially in peach seedlings (Fig. 5, Fig. 6, Fig. 8; Fig. S4, Fig. S5). This result is reminiscent of PEST sequence phosphorylation in the tymovirus *Turnip yellow mosaic virus* (TYMV) 66K protein. This sequence, a conditional signal for protein degradation, is located in the protein N-terminal region; its phosphorylation leads to a reduction in 66K accumulation and disturbs viral replication (Jakubiec and Jupin, 2007; Jakubiec *et al.*, 2006). No PEST motifs were soundly predicted by the Epestfind software at sequences surrounding the PPV CP phosphorylation sites or in other potyviral CP sequences. However, the N-terminal region of PPV CP meets some of the requirements assigned to standard PEST motifs: it is an unstructured region, rich in proline, Thr and Ser residues. Moreover, the CP of the potyvirus PVA is targeted by a ubiquitin-proteasome degradation pathway, which limits the amount of CP during early infection stages (Besong-Ndika *et al.*, 2015; Hafrén *et al.*, 2010; Lõhmus *et al.*, 2017). A similar mechanism might be hypothesized by which phosphorylation would reduce protein stability and thus regulate PPV CP accumulation. In agreement with a relationship between PPV CP phosphorylation and susceptibility to proteolytic degradation, we have observed that emulation of N-terminal phosphorylation increases PPV CP instability when incubated in crude extracts of infected tissue (Fig. 9). However, we cannot discriminate between a direct effect of the phosphorylated-like condition on susceptibility to proteolytic degradation and an indirect effect by affecting virion structure.

The finding that the fitness of the phosphorylation-deficient h-4SA mutant, although much higher than that of the phosphorylation-mimicking h-4SD mutant, was lower than that of the wild-type virus (Fig. 7 and Fig. S6) supports the view that phosphorylation at the N-terminal side of PPV CP has a regulatory role rather than being a simple plant antiviral response. *O*-GlcNAcylation is proposed to have an effect opposite to that of phosphorylation, thus blocking protein degradation (Cheng *et al.*, 2000), and depletion of *O*-GlcNAc target sites makes PPV CP more sensitive to proteolytic degradation (Pérez *et al.*, 2013). Although we detected only limited crosstalk between phosphorylation and *O*-GlcNAcylation of PPV CP, these PTMs might thus act in concert to maintain appropriate CP levels at each step of viral infection.

Phosphomimicking at positions 25, 81 and/or 101 appears to contribute to the low infection efficiency of the h-4SD mutant. Potentially adaptive mutations in the h-4SD progeny affected position 118, but not positions 25, 81 and 101, and single mutations S25D, S81D and S101D were stable, whereas Asp-118 readily evolved to Asn. All of these findings highlight the distinct disruptive effect of mimicking phosphorylation at position 118. It is intriguing that, although phosphomimicry at position 118 appears to be deleterious, our MS analyses of purified virions only detected phosphorylated species of peptides containing Ser-118 (Tables S1 and S2). This could indicate that, although phosphorylation at Ser-118 facilitates virion assembly, non-phosphorylated Ser-118 is needed for the optimal function of non-assembled CP, probably at the early stages of viral infection. Further analyses are nonetheless needed to rule out a lack of detection of species with non-phosphorylated Ser-118 as a result of technical limitations.

Neither the single h-S118D mutant nor the multiple h-4SD mutant reverted to forms with the original Ser in position 118, probably because this would require two nucleotide changes. In contrast, mutations to Asn in this position occurred in h-S118D progeny and to Asn or Gly in those of the h-4SD virus. This indicates that very different amino acids (Ser, Gly, Ala, Asn) are suitable for position 118, and that the negative charge emulating phosphorylation is likely to disturb CP function. The overall net charge of the

N-terminal region of the potyviral CP has been shown to affect virus infectivity (Kimalov *et al.*, 2004). The fact that single S25D, S81D and S101D mutations caused no noticeable fitness decrease suggests that defects of viruses bearing the S118D mutation are not simply the result of a non-specific reduction in protein net charge. Indeed, some potentially adaptive mutations introduced in h-4SD did not affect any of the four residues changed to Asp. One of them, P67S, is in the protein N-terminal region near the phosphoacceptor residues. A polymorphism at the adjacent position (Gly/Arg at position 66) determines phosphorylation of a still uncharacterized site in the CP of a Rec strain PPV isolate (Šubr *et al.*, 2010) (see Fig. S8). The other three secondary mutations in the h-4SD progeny that did not target Asp-118 mapped to a small segment of the C-terminal part of the CP core region, and affected quite different amino acids (R237Q, T254K and Y266F). Of note, our preliminary results show peptide species possibly phosphorylated at Thr-254 (not shown). In any case, these distant changes can compensate for the effect of the h-4SD Ser-to-Asp mutations, which is in agreement with the prediction that the CP N- and C-terminal regions interact in the potyviral virion (Baratova *et al.*, 2001).

Ivanov *et al.* (2001, 2003) reported phosphorylation of the potyvirus PVA CP at Thr-242 or, alternatively, at Thr-243, which coincides with the highly conserved PPV Thr-304 when both protein sequences are aligned (Fig. S8). Although phosphorylation of some viral proteins does not appear to affect RNA binding (Hu *et al.*, 2015; Zhao *et al.*, 2015), in other cases, the ability to bind RNA is conditioned by the phosphorylation status (Hoover *et al.*, 2016; Hung *et al.*, 2014; Stork *et al.*, 2005; Vijayapalani *et al.*, 2012); finally, both circumstances can coexist in the same protein (Makarov *et al.*, 2012). Phosphorylation at Thr-242 down-regulates PVA CP RNA-binding activity (Ivanov *et al.*, 2001). Prevention or mimicking of phosphorylation at Thr-242/3 disturbs PVA movement, which suggests that phosphorylation at these residues prevents premature virion formation at early stages of infection; later dephosphorylation would enhance CP binding to viral RNA and the assembly of viral particles (Ivanov *et al.*, 2003; Lõhmus *et al.*, 2017). The absence of peptides phosphorylated in Thr-304, the PPV residue that aligns with PVA Thr-243, in purified PPV virions in our MS analyses would appear to agree with this hypothesis, although further analyses of non-assembled CP early in infection would be needed for validation.

Protein kinase CK2 phosphorylates PVA CP at Thr-242/3 (Ivanov *et al.*, 2003; Lõhmus *et al.*, 2017), and the PPV CP Thr-304 environment conserves the CK2 consensus sequence [S/T]XX[D/E] (Fig. S8). This sequence is not found near the phosphoacceptor sites of PPV CP identified here, suggesting that more than one protein kinase is involved in potyviral CP phosphorylation. Phosphorylation with two independent roles in the same viral protein has been reported for the RNA-dependent RNA polymerase of TYMV; phosphorylation at its N-terminal PEST sequence regulates protein stability (see above), whereas phosphorylation in the palm domain critically affects its function in RNA replication (Jakubiec *et al.*, 2006). We propose that, although the RNA-binding ability and virion assembly potential of potyviral CP are controlled by phosphorylation at the C-terminal side, phosphorylation and *O*-GlcNAcylation at the N-terminal side regulate its susceptibility to degradation by the ubiquitin-proteasome system. The results reported here not only help us to understand the role of phosphorylation in the regulation of viral infection, but also provide essential clues to defining the interplay between phosphorylation and *O*-GlcNAcylation in the PTMs of proteins in plants.

EXPERIMENTAL PROCEDURES

Viral cDNA clones

Mutations that affect phosphorylation target sites at the PPV CP N-terminal side were engineered into PPV full-length cDNA clones pICPPV-NK-lGFP or pICPPV-NK-GFP, which derive from the PPV-R isolate (Fernández-Fernández *et al.*, 2001; Pérez *et al.*, 2013) and are suited for the infection of herbaceous plants (denoted 'h'). Mutations were also engineered in pICPPV-5′BD-GFP, a chimeric clone derived from pICPPV-NK-GFP and cDNA from a D-type PPV isolate that efficiently infects *Prunus* plants (Salvador *et al.*, 2008) (denoted 'sf'). Details of the cloning strategy are described in Methods S1 (see Supporting Information).

Plants and viral inoculation

Young plants of *N. benthamiana* and *P. persica* cv. GF305 (four- to six-leaf stage) were inoculated by bombardment with microgold particles coated with DNA of pICPPV-NK-lGFP- or pICPPV-5′BD-GFP-derived plasmids using a Helios gene gun (Bio-Rad, Hercules, CA, USA) (López-Moya and García, 2000) as explained in Methods S1. Alternatively, *N. benthamiana* plants (four- to six-leaf stage) were inoculated manually with PPV cDNA clones by rubbing with 5 μL of plasmid DNA (1 μg/μL), three leaves per plant, using carborundum as abrasive agent. Crude extracts of PPV-infected *N. benthamiana* leaves (1 g leaf tissue in 2 mL of 5 mM sodium phosphate, pH 7.2) were used to further inoculate *N. benthamiana*, *N. clevelandii* and *C. foetidum* plants by rubbing three leaves per plant, using carborundum.

The *N. benthamiana* transgenic line irSEC-b2–4 (SEC-b2), in which the *SEC* gene was down-regulated by RNAi, was obtained by transformation with an inverted-repeat sequence (360 bp) of the *N. benthamiana SEC-b2* gene, homologous to *A. thaliana SEC* (Pérez, 2014).

Plants were cultured in a glasshouse with 16 h of light by supplementary illumination and kept at 19–24 °C.

Assessment of viral infection and CP stability

Virus infection was first assessed by monitoring PPV-expressed GFP under a long-wavelength UV lamp (Black Ray model B-100 AP; Ultra-Violet Products, Upland, CA, USA) or under a Leica MZ FLIII stereomicroscope (Leica Microsystems, Wetzlar, Germany) with excitation and barrier filters of 480/40 nm and 510 nm, respectively. Images were acquired with Nikon D1X (for UV) and Olympus DP70 (for fluorescence) digital cameras (both Tokyo, Japan).

PPV accumulation was determined by Western blot analysis as described by Pérez *et al.* (2013). To detect CP *O*-GlcNAcylation qualitatively in Fig. 2, purified PPV virions were subjected to sodium dodecylsulfate-polyacrylamide gel electrophoresis (SDS-PAGE) and subsequent electroblotting to nitrocellulose membranes, and immunodetected with an *O*-GlcNAc-specific monoclonal antibody (CTD110.6, 1:2000; Sigma-Aldrich, St. Louis, MO, USA) using a horseradish peroxidase (HRP)-conjugated sheep anti-mouse immunoglobulin antibody (GE Healthcare Life Science, Marlborough, MA, USA) as secondary reagent (1 : 20 000). Immunostained proteins were visualized by enhanced chemiluminescence detection with a LiteAblot kit (Euroclone, Milano, Italy). Blots used to detect the anti-*O*-GlcNAc reaction were treated with Reblot Plus Strong (Millipore, Temecula, CA, USA) prior to CP immunodetection. Ponceau red staining was used to check the total protein content of the samples.

The preparation of cell-free extracts and the assays of CP stability were carried out as described previously (Valli *et al.*, 2014).

For genome characterization of viral progeny, appropriate cDNA fragments were amplified by RT-PCR from total RNA purified from infected leaves with a FavorPrep Plant Total RNA Purification Mini-Kit (Favorgen Biotech, Pingtung, Taiwan) or by IC-RT-PCR directly from infected tissue (Pérez *et al.*, 2013). Primers used for amplification were oligo 2429 and SM13-lGFP for most h-series viruses, and 2429 and 80 for sf-series and h-S81D (Table S5, see Supporting Information). Sequencing analysis of the amplified fragments covering the whole CP sequence was performed by Macrogen Europe (Amsterdam, Netherlands) using primers SM30-F-ext and 55 (Table S5).

Proteomic approaches

PPV virions for proteomic analyses were purified from infected *N. benthamiana* plants (wild-type or SEC-b2) as described previously (Laín *et al.*, 1988), with slight modifications (Chen *et al.*, 2005).

MALDI-TOF

PPV virions were digested with 50 ng of proteomics grade trypsin (Sigma-Aldrich, St. Louis, MO, USA; 20 min, room temperature) and purified as described previously (Chen *et al.*, 2005). Eluted peptides were dried by speed-vacuum centrifugation and resuspended in a buffer containing 30% acetonitrile, 15% isopropanol and 0.5% trifluoroacetic acid. A 1-μL aliquot of each peptide mixture was deposited manually on a 384-well OptiTOF Plate (SCIEX, Framingham, MA, USA) and allowed to dry at room temperature. A 1-μL aliquot of matrix solution (10 mg/mL 2,5-dihydroxyacetophenone in 50% aqueous acetonitrile and 100 mM ammonium citrate) was then deposited onto the dried digest and allowed to dry at room temperature. After drying, the samples were analysed in an ABi 4800 MALDI TOF/TOF mass spectrometer (SCIEX) in positive ion linear mode, as described previously (Taurino *et al.*, 2014). The detection mass range was set between 1000 and 10 000 *m/z*.

ESI MS/MS

PPV virions were methanol–chloroform precipitated, reconstituted in a buffer containing 7 M urea, 2 M thiourea and 100 mM triethylammonium bicarbonate (TEAB), and, after reduction with tris(2-carboxyethyl)phosphine (TCEP) and alkylation with methyl methanethiosulfonate (MMTS), were proteolysed with Lys-C/trypsin.

For phosphopeptide enrichment, two in-house-packed micro-columns, IMAC and Oligo R3 reverse-phase, were concatenated for selective purification and sample clean-up before liquid chromatography (LC)-MS/MS analysis (Navajas *et al.*, 2011). Phosphopeptide-enriched fractions were analysed by two 1D-nano LC-MS/MS systems, with one LC coupled to a TripleTOF analyser and the other to an ion trap mass spectrometer. Details of these techniques are given in Methods S1.

For the differential proteomics iTRAQ procedure, peptides resulting from Lys-C/trypsin treatment were labelled using the iTRAQ 4-plex kit (SCIEX), as described previously (Ciordia *et al.*, 2016), following this scheme: WT biological replica 1, tag-114; SEC-b2 biological replica 1, tag-115; WT biological replica 2, tag-116; SEC-b2 biological replica 2, tag-117. Labelled samples were pooled, dried and desalted using a SEP-PAK C18 Cartridge (WATERS, Milford, MA, USA), and subjected to nanoLC-ESI-MS/MS TripleTOF after phosphopeptide enrichment (Methods S1).

ACKNOWLEDGEMENTS

We thank C. Simón Mateo and D. Chen (Centro Nacional de Biotecnología, Madrid, Spain) for their contribution to the production of irSEC-b2–4 transgenic lines, and C. Mark for editorial assistance. M.H. was a recipient of a Training of Research Personnel contract from the Spanish Ministry of Economy, Industry and Competitiveness (MINECO). J.A.G., S.M.-T. and J.d.J.P. conceived the initial hypothesis and the work plan; S.M.-T., J.d.J.P. and M.H. designed and performed plasmid construction and infection experiments; S.M.-T., J.d.J.P., M.H. and J.A.G. analysed the infection data; N.D.U., J.S. and D.F.H. designed and performed the initial proteomics experiments; R.N. and S.C. designed and performed the definitive proteomics experiments; S.M.-T. and J.A.G. assembled the proteomics data and wrote the paper. This work was supported by grants BIO2013–49053-R, BIO2016–80572-R and Plant KBBE PCIN-2013-056 from Spanish Ministry of Economy and Competitiveness (MEC) to J.A.G., Plataforma de Recursos Biomoleculares y Bioinformáticos-Instituto de Salud Carlos III (PRB2-ISCIII) to the Centro Nacional de Biotecnología (CNB) Proteomics Facility and National Institutes of Health (NIH) GM 037537 to D.F.H.

REFERENCES

Baratova, L.A., Efimov, A.V., Dobrov, E.N., Fedorova, N.V., Hunt, R., Badun, G.A., Ksenofontov, A.L., Torrance, L. and Järvekülg, L. (2001) In situ spatial organization of Potato virus A coat protein subunits as assessed by tritium bombardment. *J. Virol.* **75**, 9696–9702.

Baratova, L.A., Fedorova, N.V., Dobrov, E.N., Lukashina, E.V., Kharlanov, A.N., Nasonov, V.V., Serebryakova, M.V., Kozlovsky, S.V., Zayakina, O.V. and Rodionova, N.P. (2004) N-terminal segment of potato virus X coat protein subunits is glycosylated and mediates formation of a bound water shell on the virion surface. *Eur. J. Biochem.* **271**, 3136–3145.

Besong-Ndika, J., Ivanov, K.I., Hafrèn, A., Michon, T. and Mäkinen, K. (2015) Cotranslational coat protein-mediated inhibition of potyviral RNA translation. *J. Virol.* **89**, 4237–4248.

Butkinaree, C., Park, K. and Hart, G.W. (2010) O-linked β-*N*-acetylglucosamine (*O*-GlcNAc): extensive crosstalk with phosphorylation to regulate signaling and transcription in response to nutrients and stress. *Biochim. Biophys. Acta*, **1800**, 96–106.

Ciordia, S., Robertson, L., Arcos, S.C., González, M.R., Mena, M.D.C., Zamora, P., Vieira, P., Abrantes, I., Mota, M., Castagnone-Sereno, P. and Navas, A. (2016) Protein markers of *Bursaphelenchus xylophilus* Steiner & Buhrer, 1934 (Nickle, 1970) populations using quantitative proteomics and character compatibility. *Proteomics*, **16**, 1006–1014.

Comer, F.I. and Hart, G.W. (2000) *O*-Glycosylation of nuclear and cytosolic proteins. Dynamic interplay between *O*-GlcNAc and *O*-phosphate. *J. Biol. Chem.* **275**, 29 179–29 182.

Champagne, J., Laliberté-Gagné, M.E. and Leclerc, D. (2007) Phosphorylation of the termini of *Cauliflower mosaic virus* precapsid protein is important for productive infection. *Mol. Plant–Microbe Interact.* **20**, 648–658.

Chen, D., Juárez, S., Hartweck, L., Alamillo, J.M., Simón-Mateo, C., Pérez, J.J., Fernández-Fernández, M.R., Olszewski, N.E. and García, J.A. (2005) Identification of secret agent as the *O*-GlcNAc transferase that participates in Plum pox virus infection. *J. Virol.* **79**, 9381–9387.

Cheng, X., Cole, R.N., Zaia, J. and Hart, G.W. (2000) Alternative O-glycosylation/O-phosphorylation of the murine estrogen receptor β. *Biochemistry (Moscow)*, **39**, 11 609–11 620.

Delporte, A., Zaeytijd, J.D., Storme, N.D., Azmi, A., Geelen, D., Smagghe, G., Guisez, Y. and Van Damme, E.J.M. (2014) Cell cycle-dependent O-GlcNAc modification of tobacco histones and their interaction with the tobacco lectin. *Plant Physiol. Biochem.* **83**, 151–158.

Fernández-Fernández, M.R., Mouriño, M., Rivera, J., Rodríguez, F., Plana-Durán, J. and García, J.A. (2001) Protection of rabbits against rabbit hemorrhagic disease virus by immunization with the VP60 protein expressed in plants with a potyvirus-based vector. *Virology*, **280**, 283–291.

Fernández-Fernández, M.R., Camafeita, E., Bonay, P., Méndez, E., Albar, J.P. and García, J.A. (2002) The capsid protein of a plant single-stranded RNA virus is modified by *O*-linked *N*-acetylglucosamine. *J. Biol. Chem.* **277**, 135–140.

García, J.A., Glasa, M., Cambra, M. and Candresse, T. (2014) *Plum pox virus* and sharka: a model potyvirus and a major disease. *Mol. Plant Pathol.* **15**, 226–241.

Hafrén, A., Hofius, D., Rönnhölm, G., Sonnewald, U. and Mäkinen, K. (2010) HSP70 and its cochaperone CPIP promote potyvirus infection in *Nicotiana benthamiana* by regulating viral coat protein functions. *Plant Cell*, **22**, 523–535.

Hagiwara-Komoda, Y., Choi, S.H., Sato, M., Atsumi, G., Abe, J., Fukuda, J., Honjo, M.N., Nagano, A.J., Komoda, K., Nakahara, K.S., Uyeda, I. and Naito, S. (2016) Truncated yet functional viral protein produced *via* RNA polymerase slippage implies underestimated coding capacity of RNA viruses. *Sci. Rep.* **6**, 21 411.

Hahne, H., Sobotzki, N., Nyberg, T., Helm, D., Borodkin, V.S., van Aalten, D.M.F., Agnew, B. and Kuster, B. (2013) Proteome wide purification and identification of *O*-GlcNAc-modified proteins using click chemistry and mass spectrometry. *J. Proteome Res.* **12**, 927–936.

Hart, G.W. (1997) Dynamic O-linked glycosylation of nuclear and cytoskeletal proteins. *Annu. Rev. Biochem.* **66**, 315–335.

Hart, G.W., Slawson, C., Ramirez-Correa, G. and Lagerlof, O. (2011) Cross talk between O-GlcNAcylation and phosphorylation: roles in signaling, transcription, and chronic disease. *Annu. Rev. Biochem.* **80**, 825–858.

Hartweck, L.M., Scott, C.L. and Olszewski, N.E. (2002) Two *O*-Linked *N*-acetylglucosamine transferase genes of *Arabidopsis thaliana* L. Heynh. have overlapping functions necessary for gamete and seed development. *Genetics*, **161**, 1279–1291.

Hoover, H.S., Wang, J.C.-Y., Middleton, S., Ni, P., Zlotnick, A., Vaughan, R.C. and Kao, C.C. (2016) Phosphorylation of the Brome mosaic virus capsid regulates the timing of viral infection. *J. Virol.* **90**, 7748–7760.

Hu, Y., Li, Z., Yuan, C., Jin, X., Yan, L., Zhao, X., Zhang, Y., Jackson, A.O., Wang, X., Han, C., Yu, J. and Li, D. (2015) Phosphorylation of TGB1 by protein kinase CK2 promotes barley stripe mosaic virus movement in monocots and dicots. *J. Exp. Bot.* **66**, 4733–4747.

Hung, C.J., Huang, Y.W., Liou, M.R., Lee, Y.C., Lin, N.S., Meng, M., Tsai, C.H., Hu, C.C. and Hsu, Y.H. (2014) Phosphorylation of coat protein by protein kinase CK2 regulates cell-to-cell movement of *Bamboo mosaic virus* through modulating RNA binding. *Mol. Plant–Microbe Interact.* **27**, 1211–1225.

Ivanov, K.I., Puustinen, P., Merits, A., Saarma, M. and Mäkinen, K. (2001) Phosphorylation down-regulates the RNA binding function of the coat protein of Potato virus A. *J. Biol. Chem.* **276**, 13 530–13 540.

Ivanov, K.I., Puustinen, P., Gabrenaite, R., Vihinen, H., Rönnstrand, L., Valmu, L., Kalkkinen, N. and Mäkinen, K. (2003) Phosphorylation of the potyvirus capsid protein by protein kinase CK2 and its relevance for virus infection. *Plant Cell*, **15**, 2124–2139.

Jakubiec, A. and Jupin, I. (2007) Regulation of positive-strand RNA virus replication: the emerging role of phosphorylation. *Virus Res.* **129**, 73–79.

Jakubiec, A., Tournier, V., Drugeon, G., Pflieger, S., Camborde, L., Vinh, J., Héricourt, F., Redeker, V. and Jupin, I. (2006) Phosphorylation of viral RNA-dependent RNA polymerase and its role in replication of a plus-strand RNA virus. *J. Biol. Chem.* **281**, 21 236–21 249.

Kearse, M., Moir, R., Wilson, A., Stones-Havas, S., Cheung, M., Sturrock, S., Buxton, S., Cooper, A., Markowitz, S., Duran, C., Thierer, T., Ashton, B., Meintjes, P. and Drummond, A. (2012) Geneious Basic: an integrated and extendable desktop software platform for the organization and analysis of sequence data. *Bioinformatics*, **28**, 1647–1649.

Kim, Y.C., Udeshi, N.D., Balsbaugh, J.L., Shabanowitz, J., Hunt, D.F. and Olszewski, N.E. (2011) *O*-GlcNAcylation of the *Plum pox virus* capsid protein catalyzed by SECRET AGENT: characterization of *O*-GlcNAc sites by electron transfer dissociation mass spectrometry. *Amino Acids*, **40**, 869–876.

Kimalov, B., Gal-On, A., Stav, R., Belausov, E. and Arazi, T. (2004) Maintenance of coat protein N-terminal net charge and not primary sequence is essential for zucchini yellow mosaic virus systemic infectivity. *J. Gen. Virol.* **85**, 3421–3430.

Laín, S., Riechmann, J.L., Méndez, E. and García, J.A. (1988) Nucleotide sequence of the 3′ terminal region of plum pox potyvirus RNA. *Virus Res.* **10**, 325–342.

Lee, J.Y. and Lucas, W.J. (2001) Phosphorylation of viral movement proteins–regulation of cell-to-cell trafficking. *Trends Microbiol.* **9**, 5–8.

Link, K., Vogel, F. and Sonnewald, U. (2011) PD trafficking of potato leaf roll virus movement protein in Arabidopsis depends on site-specific protein phosphorylation. *Front. Plant Sci.* **2**, 1–10.

Lõhmus, A., Hafrén, A. and Mäkinen, K. (2017) Coat protein regulation by CK2, CPIP, HSP70 and CHIP is required for Potato virus A replication and coat protein accumulation. *J. Virol.* **91**, 1–38.

López-Moya, J.J. and García, J.A. (2000) Construction of a stable and highly infectious intron-containing cDNA clone of plum pox potyvirus and its use to infect plants by particle bombardment. *Virus Res.* **68**, 99–107.

Makarov, V.V., Iconnikova, A.Y., Guseinov, M.A., Vishnichenko, V.K. and Kalinina, N.O. (2012) *In vitro* phosphorylation of the N-terminal half of hordeivirus movement protein. *Biochemistry (Moscow)*, **77**, 1072–1081.

Módena, N.A., Zelada, A.M., Conte, F. and Mentaberry, A. (2008) Phosphorylation of the TGBp1 movement protein of *Potato virus X* by a *Nicotiana tabacum* CK2-like activity. *Virus Res.* **137**, 16–23.

Navajas, R., Paradela, A. and Albar, J.P. (2011) Immobilized metal affinity chromatography/reversed-phase enrichment of phosphopeptides and analysis by CID/ETD tandem mass spectrometry. *Methods Mol. Biol.* **681**, 337–348.

Olspert, A., Chung, B.Y.W., Atkins, J.F., Carr, J.P. and Firth, A.E. (2015) Transcriptional slippage in the positive-sense RNA virus family *Potyviridae*. *EMBO Rep.* **16**, 995–1004.

Olszewski, N.E., West, C.M., Sassi, S.O. and Hartweck, L.M. (2010) O-GlcNAc protein modification in plants: evolution and function. *Biochim. Biophys. Acta*, **1800**, 49–56.

Pérez, J.D.J. (2014) *Caracterización de la modificación por O-GlcNAc de la proteína de la cápside del potyvirus Plum pox virus y su relevancia par la infección viral.* PhD thesis. Departamento de Biología Molecular, Universidad Autónoma de Madrid, Madrid, Spain.

Pérez, J.D.J., Juárez, S., Chen, D., Scott, C.L., Hartweck, L.M., Olszewski, N.E. and García, J.A. (2006) Mapping of two *O*-GlcNAc modification sites in the capsid protein of the potyvirus *Plum pox virus*. *FEBS Lett.* **580**, 5822–5828.

Pérez, J.D.J., Udeshi, N.D., Shabanowitz, J., Ciordia, S., Juárez, S., Scott, C.L., Olszewski, N.E., Hunt, D.F. and García, J.A. (2013) *O*-GlcNAc modification of the coat protein of the potyvirus *Plum pox virus* enhances viral infection. *Virology*, **442**, 122–131.

Puustinen, P., Rajamäki, M.L., Ivanov, K.I., Valkonen, J.P.T. and Mäkinen, K. (2002) Detection of the potyviral genome-linked protein VPg in virions and its phosphorylation by host kinases. *J. Virol.* **76**, 12 703–12 711.

Revers, F. and García, J.A. (2015) Molecular biology of potyviruses. *Adv. Virus Res.* **92**, 101–199.

Rodamilans, B., Valli, A., Mingot, A., San León, D., Baulcombe, D., López-Moya, J.J. and García, J.A. (2015) RNA polymerase slippage as a mechanism for the production of frameshift gene products in plant viruses of the *Potyviridae* family. *J. Virol.* **89**, 6965–6967.

Salvador, B., Delgadillo, M.O., Saénz, P., García, J.A. and Simón-Mateo, C. (2008) Identification of *Plum pox virus* pathogenicity determinants in herbaceous and woody hosts. *Mol. Plant–Microbe Interact.* **21**, 20–29.

Samuilova, O., Santala, J. and Valkonen, J.P.T. (2013) Tyrosine phosphorylation of the triple gene block protein 3 regulates cell-to-cell movement and protein interactions of *Potato mop-top virus*. *J. Virol.* **87**, 4313–4321.

Scott, C.L., Hartweck, L.M., Pérez, J.D.J., Chen, D., García, J.A. and Olszewski, N.E. (2006) SECRET AGENT, an *Arabidopsis thaliana O*-GlcNAc transferase, modifies the *Plum pox virus* capsid protein. *FEBS Lett.* **580**, 5829–5835.

Schouppe, D., Ghesquière, B., Menschaert, G., De Vos, W.H., Bourque, S., Trooskens, G., Proost, P., Gevaert, K. and Van Damme, E.J.M. (2011) Interaction of the tobacco lectin with histone proteins. *Plant Physiol.* **155**, 1091–1102.

Shapka, N., Stork, J. and Nagy, P.D. (2005) Phosphorylation of the p33 replication protein of *Cucumber necrosis tombusvirus* adjacent to the RNA binding site affects viral RNA replication. *Virology*, **343**, 65–78.

Slawson, C. and Hart, G.W. (2003) Dynamic interplay between O-GlcNAc and O-phosphate: the sweet side of protein regulation. *Curr. Opin. Struct. Biol.* **13**, 631–636.

Steiner, E., Efroni, I., Gopalraj, M., Saathoff, K., Tseng, T.S., Kieffer, M., Eshed, Y., Olszewski, N. and Weiss, D. (2012) The *Arabidopsis O*-linked *N*-acetylglucosamine transferase SPINDLY interacts with class I TCPs to facilitate cytokinin responses in leaves and flowers. *Plant Cell*, **24**, 96–108.

Stork, J., Panaviene, Z. and Nagy, P.D. (2005) Inhibition of in vitro RNA binding and replicase activity by phosphorylation of the p33 replication protein of *Cucumber necrosis tombusvirus*. *Virology*, **343**, 79–92.

Šubr, Z. and Glasa, M. (2013) Unfolding the secrets of plum pox virus: from epidemiology to genomics. *Acta Virol.* **57**, 217–228.

Šubr, Z., Ryšlavá, H. and Kollerová, E. (2007) Electrophoretic mobility of the capsid protein of the Plum pox virus strain PPV-Rec indicates its partial phosphorylation. *Acta Virol.* **51**, 135–138.

Šubr, Z.W., Kamencayová, M., Nováková, S., Nagyová, A., Nosek, J. and Glasa, M. (2010) A single amino acid mutation alters the capsid protein electrophoretic double-band phenotype of the *Plum pox virus* strain PPV-Rec. *Arch. Virol.* **155**, 1151–1155.

Taoka, K., Ham, B.K., Xoconostle-Cázares, B., Rojas, M.R. and Lucas, W.J. (2007) Reciprocal phosphorylation and glycosylation recognition motifs control NCAPP1 interaction with pumpkin phloem proteins and their cell-to-cell movement. *Plant Cell*, **19**, 1866–1884.

Taurino, M., Abelenda, J.A., Río-Alvarez, I., Navarro, C., Vicedo, B., Farmaki, T., Jiménez, P., García-Agustín, P., López-Solanilla, E., Prat, S., Rojo, E., Sánchez-Serrano, J.J. and Sanmartín, M. (2014) Jasmonate-dependent modifications of the pectin matrix during potato development function as a defense mechanism targeted by *Dickeya dadantii* virulence factors. *Plant J.* **77**, 418–429.

Trinidad, J.C., Barkan, D.T., Gulledge, B.F., Thalhammer, A., Sali, A., Schoepfer, R. and Burlingame, A.L. (2012) Global identification and characterization of both *O*-GlcNAcylation and phosphorylation at the murine synapse. *Mol. Cell. Proteomics*, **11**, 215–229.

Valli, A., Gallo, A., Calvo, M., Pérez, J.D.J. and García, J.A. (2014) A novel role of the potyviral helper component proteinase contributes to enhance the yield of viral particles. *J. Virol.* **17**, 9808–9818.

Vijayapalani, P., Chen, J.C.F., Liou, M.R., Chen, H.C., Hsu, Y.H. and Lin, N.S. (2012) Phosphorylation of bamboo mosaic virus satellite RNA (satBaMV)-encoded protein P20 downregulates the formation of satBaMV-P20 ribonucleoprotein complex. *Nucleic Acids Res.* **40**, 638–649.

Wang, J., Torii, M., Liu, H., Hart, G.W. and Hu, Z.Z. (2011) dbOGAP – an integrated bioinformatics resource for protein O-GlcNAcylation. *BMC Bioinformatics*, **12**, 91.

Wells, L., Vosseller, K. and Hart, G.W. (2001) Glycosylation of nucleocytoplasmic proteins: signal transduction and O-GlcNAc. *Science*, **291**, 2376–2378.

Xiao, J., Xu, S., Li, C., Xu, Y., Xing, L., Niu, Y., Huan, Q., Tang, Y., Zhao, C., Wagner, D., Gao, C. and Chong, K. (2014) *O*-GlcNAc-mediated interaction between VER2 and TaGRP2 elicits *TaVRN1* mRNA accumulation during vernalization in winter wheat. *Nat. Commun.* **5**, 4572.

Xing, L., Li, J., Xu, Y., Xu, Z. and Chong, K. (2009) Phosphorylation modification of wheat lectin VER2 is associated with vernalization-induced O-GlcNAc signaling and intracellular motility. *PLoS One*, **4**, e4854.

Xu, S.-L., Chalkley, R.J., Maynard, J.C., Wang, W., Ni, W., Jiang, X., Shin, K., Cheng, L., Savage, D., Hühmer, A.F.R., Burlingame, A.L. and Wang, Z.-Y. (2017) Proteomic analysis reveals O-GlcNAc modification on proteins with key regulatory functions in Arabidopsis. *Proc. Natl. Acad. Sci. USA*, **114**, E1536–E1543.

Zeidan, Q. and Hart, G.W. (2010) The intersections between *O*-GlcNAcylation and phosphorylation: implications for multiple signaling pathways. *J. Cell Sci.* **123**, 13–22.

Zentella, R., Hu, J., Hsieh, W.P., Matsumoto, P.A., Dawdy, A., Barnhill, B., Oldenhof, H., Hartweck, L.M., Maitra, S., Thomas, S.G., Cockrell, S., Boyce, M., Shabanowitz, J., Hunt, D.F., Olszewski, N.E. and Sun, T.P. (2016) *O*-GlcNAcylation of master growth repressor DELLA by SECRET AGENT modulates multiple signaling pathways in *Arabidopsis*. *Genes Dev.* **30**, 164–176.

Zhao, X., Wang, X., Dong, K., Zhang, Y., Hu, Y., Zhang, X., Chen, Y., Wang, X., Han, C., Yu, J. and Li, D. (2015) Phosphorylation of *Beet black scorch virus* coat protein by PKA is required for assembly and stability of virus particles. *Sci. Rep.* **5**, 11 585.

SUPPORTING INFORMATION

Additional Supporting Information may be found in the online version of this article at the publisher's web-site:

Methods S1 Additional details with regard to the Experimental procedures section.

Fig. S1 Electron-transfer dissociation-tandem mass spectrometry (ETD-MS/MS) spectra supporting phosphorylation mapping at S81 contained in peptide [71–93], S101 in peptide [94–109] and S118 in peptide [112–121], bearing or not an oxidized methionine.

Fig. S2 Effect of decreased *O*-GlcNAcylation on the *Plum pox virus* (PPV) capsid protein (CP) phosphorylation level at serine (Ser) residues 81 and 101. The table compares the percentages of intensity values of phosphorylated species (Phos level) with all peptide species containing Ser-81 ([40–93], [60–93] and [60–95]) or Ser-101 ([94–109] and [96–109]). Values shown for each biological replica of PPV virions purified from wild-type and SEC-b2 *Nicotiana benthamiana* plants and their averages. Individual values are plotted in histograms (top).

Fig. S3 Scheme of the *Plum pox virus* (PPV) capsid protein (CP) N-terminal side showing mutations introduced into PPV full-length cDNA clones. Mutated residues are shown in red. Prefixes 'h' or 'sf' refer to constructs based on pICPPV-NK-GFP/pICPPV-NK-lGFP or pICPPV-NK-5′BD plasmids, suitable for the inoculation of herbaceous or woody hosts, respectively.

Fig. S4 Accumulation of wild-type *Plum pox virus* (PPV) and PPV mutants affected at capsid protein (CP) phosphotarget residues in *Nicotiana benthamiana* plants after inoculation by bombardment of viral cDNA. Extracts from systemically infected leaves were collected at 21 days post-inoculation (dpi), pooled and tested in PPV CP-specific immunoblot analysis. Inoculated viruses, pooled plants and extract volume loaded are indicated. Blots stained with Ponceau red showing the ribulose-1,5-bisphosphate carboxylase/oxygenase (RuBisCO) protein are included as loading control.

Fig. S5 Infection of *Nicotiana clevelandii* and *Chenopodium foetidum* plants by wild-type *Plum pox virus* (PPV) and PPV mutants affected at capsid protein (CP) phosphotarget residues. Plants were inoculated by hand rubbing with leaf extracts of previously infected *Nicotiana benthamiana* plants. (A) Images of upper uninoculated leaves of *N. clevelandii* plants infected with the indicated viruses, taken at 10 or 24 days post-inoculation (dpi), under an epifluorescence microscope. Bar, 5 mm. (B) PPV CP-specific immunoblot analysis of extracts of upper uninoculated leaves from four individual plants infected with viruses as indicated. Samples were collected at 10 and 24 dpi. Blots stained with Ponceau red showing the ribulose-1,5-bisphosphate carboxylase/oxygenase (RuBisCO) protein are included as loading control. (C) Images of inoculated leaves of *C. foetidum* plants infected with the indicated viruses, taken at 10 and 16 dpi under visible light. Bar, 10 mm.

Fig. S6 Sequence analysis of viral progeny from mixed infections with wild-type *Plum pox virus* (PPV) (h-WT) and a PPV mutant in which phosphorylation of the capsid protein (CP) at serine residues 25, 81, 101 and 118 (h-4SA) is prevented. Mixtures of extracts of *Nicotiana benthamiana* plants infected with h-4SA

and h-WT, combined at the indicated ratios, were used to inoculate *N. benthamiana* and *Nicotiana clevelandii* plants. Viruses in infected plants were identified by reverse transcription-polymerase chain reaction (RT-PCR) and sequencing of a cDNA fragment covering the CP coding region. An extract from an *N. clevelandii* plant in which h-WT and h-4SA accumulated at similar levels was used to inoculate new *N. benthamiana* and *N. clevelandii* plants, whose viral progeny were assessed as above. Chromatograms show the region of sequencing corresponding to the triplet coding for CP residues 25, 81, 101 and 118.

Fig. S7 Secondary mutations detected in the viral progeny of the *Plum pox virus* (PPV) phosphomimicking mutant h-4SD. Genome sequencing of the viral progeny of *Nicotiana benthamiana* plants infected with PPV h-4SD was assessed by reverse transcription-polymerase chain reaction (RT-PCR) and sequencing of cDNA fragments covering the complete capsid protein (CP) coding region. Sequence chromatograms show secondary mutations affecting the triplets encoding Ser-118 and Arg-237 (stars), which were detected in some of the infected plants. The unaltered sequence of triplets coding for phosphotargets Ser-25, Ser-81 and Ser-101 is also shown.

Fig. S8 Sequence alignment of capsid protein (CP) from several *Plum pox virus* (PPV) isolates of eight PPV strains. Proteins were aligned using the MUSCLE method (Edgar, 2004), integrated into the Geneious 9.1.5 software (http://www.geneious.com; Kearse *et al.*, 2012). Disagreements relative to the reference sequence of the Rankovic isolate are highlighted. Phosphotargets identified in this study (red), residues altered by potentially compensatory mutations in h-4SD progeny (blue) and the residue corresponding to the amino acid phosphorylated by CK2 kinase in the potyvirus *Potato virus A* (PVA) CP (green) (Ivanov *et al.*, 2001, 2003).

Table S1 Phosphopeptides identified by triple time-of-flight (TripleTOF) high-resolution mass spectrometry (MS) and/or electron-transfer dissociation (ETD) ion trap low-resolution MS.

Table S2 Comprehensive listing of iTRAQ (isobaric tags for relative and absolute quantitation) intensity values.

Table S3 Label-free quantification of *O*-GlcNAcylation and phosphorylation of the peptide [1–39] in wild-type and SEC-b2 *Nicotiana benthamiana* plants.

Table S4 Infectivity in *Nicotiana benthamiana* of wild-type (WT) *Plum pox virus* (PPV) and phosphomimicking PPV mutants.

Table S5 Primer list.